Ferrocene-containing polycarbosilazanes *via* the alkaline-earth catalyzed dehydrocoupling of silanes and amines

Louis J. Morris,[a,b] George R. Whittell,[b] Jean-Charles Eloi,[a] Mary F. Mahon,[a] Frank Marken,[a] Ian Manners*[,b,c] and Michael S. Hill*[,a]

[a] Department of Chemistry, University of Bath, Claverton Down, Bath BA2 7AY, United Kingdom; [b] School of Chemistry, University of Bristol, Cantock's Close, Bristol BS8 1TS, United Kingdom; [c] Department of Chemistry, University of Victoria, Victoria BC V8P 5C2, Canada

email: msh27@bath.ac.uk; imanners@uvic.ca

Abstract: We report the use of the alkaline-earth (Ae) metal-catalyzed dehydrocoupling of silanes and amines for the synthesis of novel ferrocene-containing polycarbosilazanes. The barium complex $[Ba(N(SiMe_3)_2)_2.(THF)_2]$ catalyzed the dehydrocoupling of the hydrosilane $FeCp(CpSiPhH_2)$ (**1**) with 1,4-$(H_2NCH_2)_2C_6H_4$ under mild conditions to give a polycarbosilazane with pendant ferrocene groups. The polymer could be readily crosslinked by the addition of phenylsilane to the unquenched reaction mixture. Well-defined polycarbosilazanes with ferrocene in the main chain were also obtained from the dehydrocoupling of hydrosilanes $Fe(Cp(SiPhH_2))_2$ (**3**), and $Fe(Cp(SiMe_2H))_2$ (**IX**) with 1,4-$(H(Me)NCH_2)_2C_6H_4$ and 1,4-$(H_2NCH_2)_2C_6H_4$ respectively. Crystalline monomeric analogues, $FeCp(Cp(SiPh(NHBn)_2))$ (**2**, Bn = $CH_2(C_6H_5)$), and $Fe(Cp(SiPh(NHBn)_2))_2$ (**4**), were also obtained *via* the dehydrocoupling benzylamine with **1** and **3**, respectively. The barium-catalyzed dehydrocoupling of diaminoferrocene with Ph_2SiH_2 or $Ph(Rc)SiH_2$ (**6**, Rc = $(C_5H_4)Ru(C_5H_5)$) did not result in polymer, but instead the formation of the silazane-bridged *ansa*-[3]ferrocenophanes $(Fe(\eta\text{-}C_5H_4NH)_2SiPh_2)$ (**5**) and $(Fe(\eta\text{-}C_5H_4NH)_2SiPh(Rc))$ (**7**), respectively. Both polymeric and molecular products were electrochemically investigated, and the polymers proved to be promising precursors to magnetic iron-containing ceramics in yields of up to 64%.

Introduction.

Polymers have become an indispensable part of the modern world thanks to their highly varied and useful properties, which makes them well suited to a variety of applications. The incorporation of metal atoms into macromolecules represents an attractive way to obtain polymeric materials with novel and interesting properties that complement those achievable with conventional all-organic polymers. Although metallopolymers have been the subject of

research for half a century,[1, 2] most early examples suffered from the use of poorly defined and highly reactive organometallic monomers, and were often inadequately characterised by modern standards.[3-6] During the last 25 years however, an increasing number of well-characterised metallopolymers with remarkable properties have been reported to date, [4, 7-18] with one of the most well-developed routes to metallopolymers utilizing the ring opening polymerisation (ROP) of strained ferrocenophanes. Discovered by Manners and co-workers in the early 1990s,[19] this process has enabled access to polymers of high molar mass, and afforded materials with tuneable properties through variation in the spacer, side chains, and also the formation of well-defined block copolymers with low dispersities.[20-22] The prerequisite for a strained ferrocenophane monomer, however, presents a limitation and certain polymer architectures, such as those with longer inter-ferrocene bridges or alternating sequences, are inaccessible by this route and demand an alternative approach.

Polycondensation is one of the most well-established polymerisation methodologies and it presents an attractive approach for the synthesis of novel metallopolymers due to theoretically facile and modular alteration of monomer structure and functionality. With a few notable exceptions, however, only limited success has been achieved in the synthesis of high molar mass inorganic polymers *via* a polycondensation approach.[23] This is predominantly due to a lack of efficient bond-forming reactions between well-defined monomers of sufficiently high purity. This basic requirement stems from the fundamental theory of step-growth polycondensation developed in the early 1930s by Carothers and Flory, which demands extremely high conversion and precise stoichiometry in order to obtain the requisite high molecular weights.[24, 25] The successful use of polycondensation in the synthesis of inorganic polymers, therefore, requires well-defined monomers of the necessary high purity and a reaction that is capable of forming element-element (E-E) bonds with extremely high conversion and high specificity. Catalytic dehydrocoupling is one such reaction and has been well studied with a variety of catalysts and main-group substrates, such that many different E-E and E-E' bonds can now be formed *via* both homo- and hetero-dehydrocoupling with H_2 as the sole by-product (Scheme 1).[26-29]

$$E{-}H + E'{-}H \xrightarrow{\text{Catalyst}} E{-}E' + H_2$$

Scheme 1: A general dehydrocoupling scheme.

Since hydrides are ubiquitous and readily available amongst many main group elements, dehydrocoupling has already provided a rich library of *p*-block element-containing polymers,[28, 30-33] including polysilanes,[32, 34-36] polylstannanes,[37-40] polyaminoboranes,[41-45] and polyphosphinoboranes.[42, 46-51] The application of dehydrocoupling as a route towards

ferrocene-containing polymers, however, is limited to two examples, the formation of a polyferrocenylthioether by Yamamoto and coworkers,[52] and Hey-Hawkins' pendant-ferrocene containing polyphosphinoboranes,[53] both of which are dependent on rhodium catalysis (

Scheme 2).

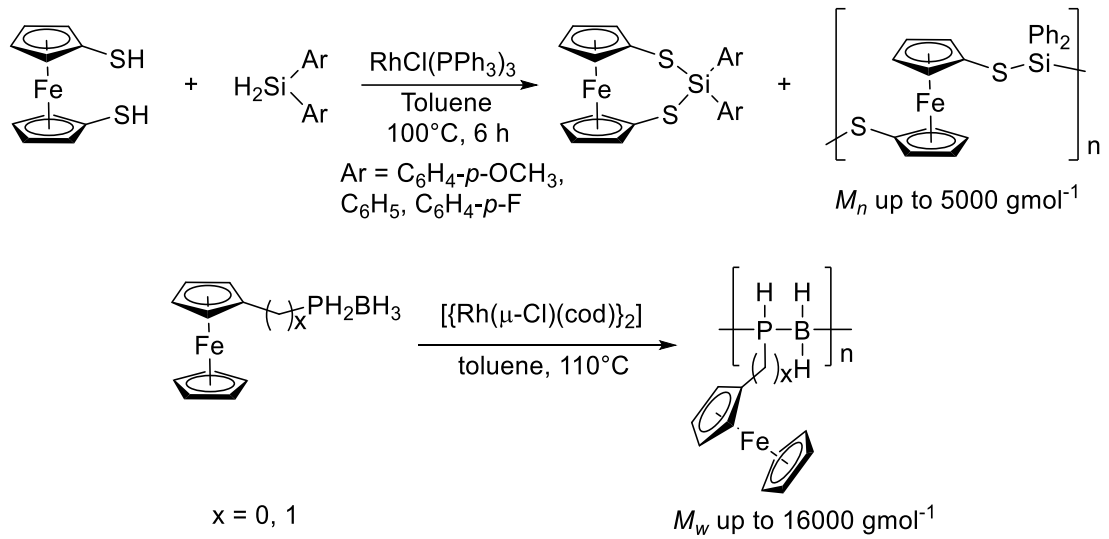

Scheme 2: Reported ferrocene-containing polymers synthesised *via* catalytic dehydrocoupling.[52, 53]

With the intention of synthesising ferrocene-containing polymers of new structure and function, we turned to the alkaline-earth (Ae) metal catalyzed dehydrocoupling of silanes and amines. Historically accessed *via* the aminolysis of chlorosilanes,[54, 55] a dehydrocoupling approach to Si-N bonds has attracted significant recent attention due to the utility of molecular and polymeric silazanes in a variety of applications including use as silylating agents,[56] bases,[57] and ceramic precursors.[58-63] A large number of catalysts have been reported for Si-N bond formation, utilising lanthanide,[64-67] actinide,[68] transition metal,[69-73] alkali metal,[74] and main group compounds,[75, 76] as well as supported metal nanoparticles[77, 78] and catalytic activation of Si-H bonds by nucleophilic fluoride attack.[59] Ae catalysis was first reported for this reaction in 2007 by Buch and Harder, who utilised a calcium azametallocyclopropane pre-catalyst.[79] Sadow and co-workers later reported the tris(oxazolinyl)boratomagnesium-catalyzed dehydrocoupling of silanes and amines,[80] while *N*-heterocyclic carbene (NHC) complexes of Mg have also been employed.[81] The reaction has also recently been the subject of extensive investigation by the groups of Hill[82] and Sarazin,[83-86] who demonstrated that simple homoleptic Ae amides $[Ae(N(SiMe_2)_2)_2.(THF)_2]$ and alkyls $[Ae(CH(SiMe_2)_2)_2.(THF)_{2\text{-}3}]$ of the heavier Ae elements (Ca, Sr, Ba) can behave as highly competent catalysts, allowing complex ligands and lengthy pre-catalyst syntheses to be avoided.

Of particular interest to this study is the utilisation of Ba-catalyzed dehydrocoupling for the preparation of polycarbosilazanes, which was recently reported by Sarazin's group.[83]

Diphenylsilane couples to *p*-xylylenediamine to yield soluble and well-characterised polycarbosilazanes of appreciable molecular weight. Furthermore, the reaction can be tailored to yield either cyclic or linear polymers by subtle alteration of reaction stoichiometry (Scheme 3).[83]

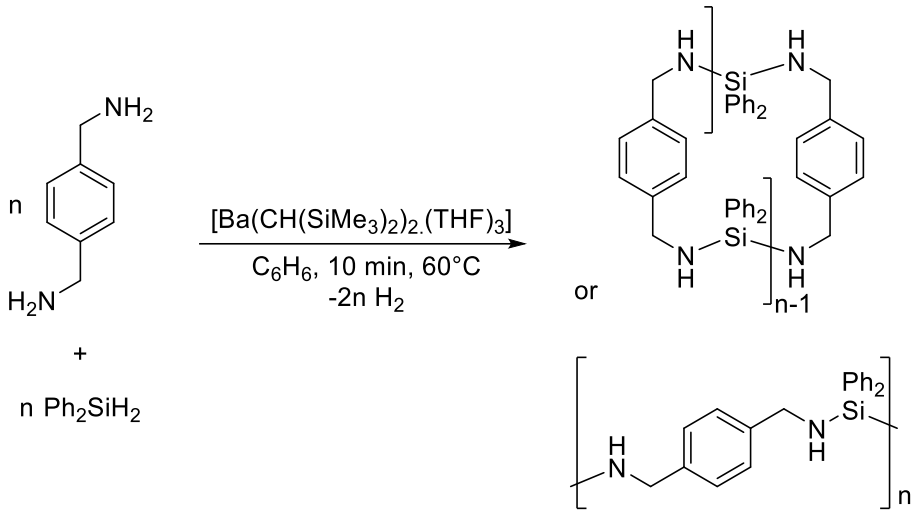

Scheme 3: The barium catalyzed dehydrocoupling of *p*-xylylenediamine and diphenylsilane to yield cyclic or linear polycarbosilazanes, as reported by Sarazin and co-workers.[83]

Despite these advances, and to the best of our knowledge, soluble, high molecular weight metallo-polycarbosilazanes are unknown. We expected that by using ferrocene-containing silanes and amines, Ae-catalyzed dehydrocoupling could be used as an effective method to access ferrocene-containing polymers *via* a condensation-polymerisation regime, thus providing access to previously unexplored polymer architectures.

Results and Discussion

Synthesis of FeCp(CpSiPhH$_2$) and reactions with benzyl amine. In the knowledge that polycarbosilazanes of respectable molecular weight could be obtained *via* the Ba-catalyzed dehydrocoupling of diphenylsilane and 1,4-$(H_2NCH_2)_2C_6H_4$,[83] we reasoned that replacement of diphenylsilane with (phenylsilyl)ferrocene (**1**) would allow straightforward access to polycarbosilazanes possessing pendant ferrocene groups.

In a model reaction, the dehydrocoupling reactivity of **1** was first investigated with benzylamine and 5 mol% [Ca(N(SiMe$_3$)$_2$)$_2$.(THF)$_2$] **I** (Scheme 4). The reaction proceeded rapidly, reaching 50% conversion after only 30 minutes at room temperature. Heating to 60°C resulted in complete conversion to the bis-coupled product **2** (Scheme 4) which crystallized in the form of pale orange needles suitable for single crystal X-ray diffraction analysis following slow evaporation of a toluene solution (Figure 1). Compound **2** crystallizes in the orthorhombic space group, *Pbcn*, with a single molecule present in the unit cell and with no close

intermolecular contacts. The heavier Ae-amides [Sr(N(SiMe$_3$)$_2$)$_2$.(THF)$_2$] **II**, and [Ba(N(SiMe$_3$)$_2$)$_2$.(THF)$_2$] **III** were even more proficient dehydrocoupling catalysts, achieving respective spectroscopic conversions of 92% and >99% to **2** after only 20 min.at room temperature at a 5 mol% loading. This observation agrees with previously reported trends in the, with higher activity correlating with an increase in Ae ionic radius, polarizability, and electropositivity.[82, 85, 86] Although Sarazin and co-workers have shown the homoleptic Ae alkyl complexes [Ae(CH(SiMe$_3$)$_2$)$_2$.(THF)$_x$] (Ae = Ca **IV**, Sr **V**, Ba **VI**, x = 2 (Ca, Sr), 3 (Ba)) to be superior Si-N dehydrocoupling catalysts than their amide analogues,[86] the synthetically less demanding amides were deemed more than adequate for the purposes of this study. For this reason, all further dehydrocoupling studies described herein utilise the Ba amide **III**, unless otherwise stated.

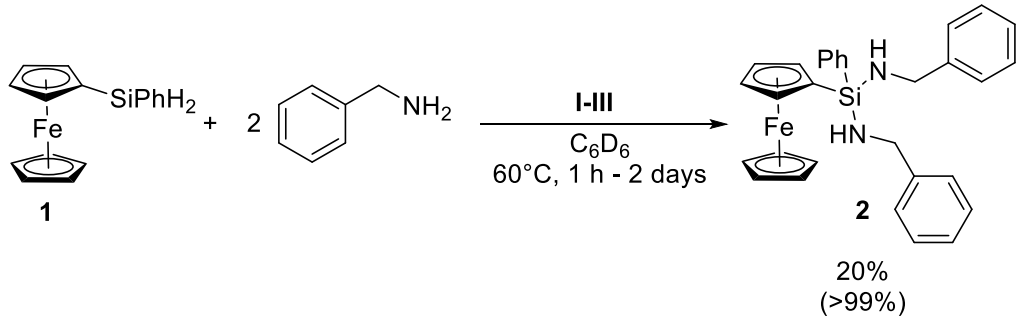

Scheme 4: The Ae-catalyzed dehydrocoupling reaction of **1** and benzylamine to give **2**. The isolated yield is given, with the yield shown in parentheses determined by ^{1}H NMR spectroscopy of the crude reaction mixture.

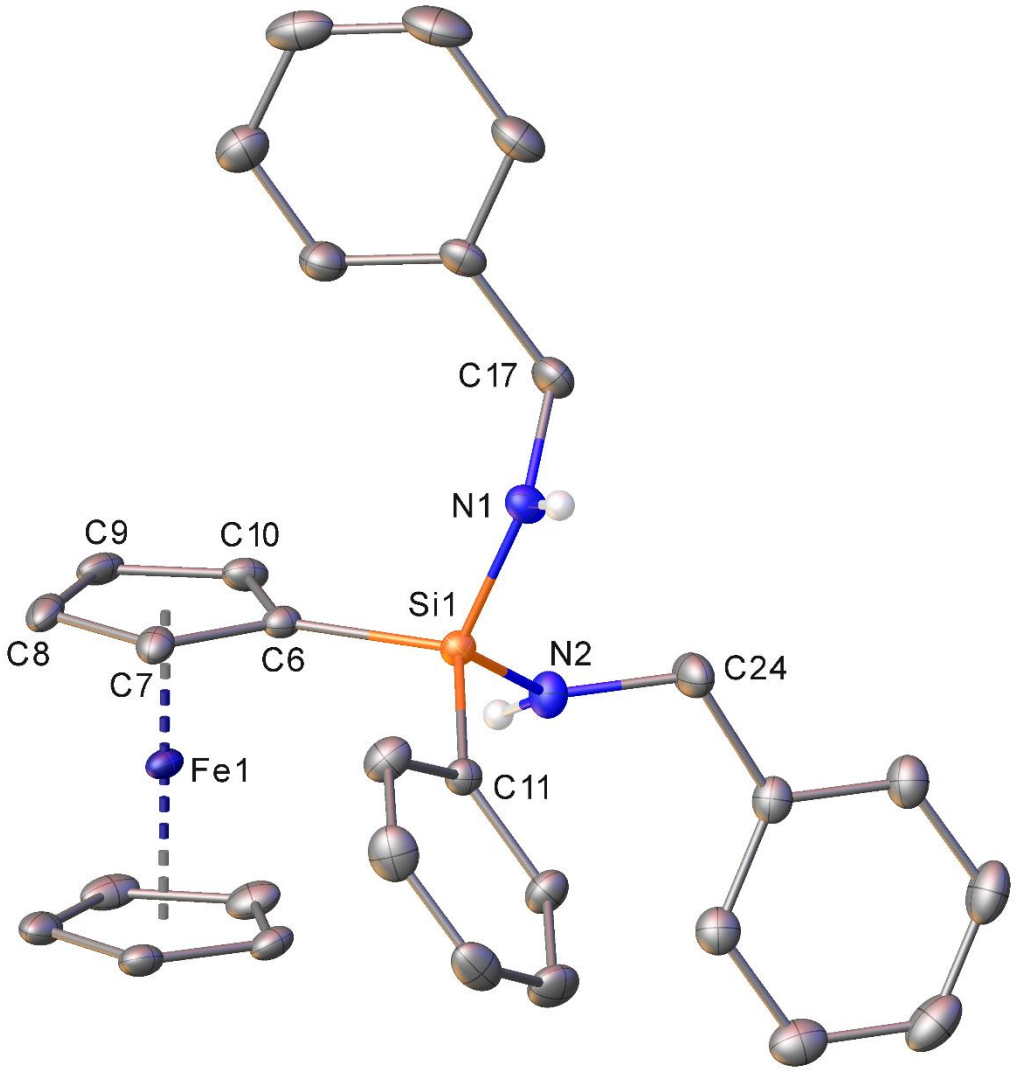

Figure 1: ORTEP representation of the X-ray crystal structure of **2**. Thermal ellipsoids are shown at the 30% probability level. Except for those bound to nitrogen, H atoms are omitted for clarity.

Synthesis and characterisation of polycarbosilazanes with ferrocene pendant to the main-chain. Encouraged by these results, dehydropolymerisation was attempted using compound **1** and the bifunctional amine 1,4-$(H_2NCH_2)_2C_6H_4$. Utilising compound **III** as a pre-catalyst at 5 mol% loading, the reaction proceeded rapidly in toluene, with immediate and vigorous release of H_2 gas (Scheme 5). After stirring at 60°C for 2 h to ensure full conversion, a pale orange solid (**P1**) was obtained following precipitation into pentane at -78°C (Scheme 5). Analysis of the product by ^{1}H NMR spectroscopy revealed a simple spectrum consistent with a polycarbosilazane backbone decorated with ferrocene groups pendant to the main chain. Although the absence of any Si-H resonances discounted the possibility of Si-terminated linear polymers, two clear resonances at δ 3.61 and 0.77 ppm were assigned as chain-end CH_2 and NH_2 groups, respectively. This enabled the average degree of polymerisation ($X_{n,\text{ end group}}$) of 22.7 and a resultant molecular weight (M_n) of ~10000 Da to be

estimated by integration (Table 1) relative to the respective mid-chain resonances at δ 4.37-4.07 (CH_2) and 1.49 ppm (NH_2). Although we cannot rule out the formation of cyclic polymer, the NMR spectra always displayed linear polymers with detectable chain-ends. This is in contrast to the analogous ferrocene-free polycarbosilazanes reported by Sarazin and co-workers, who obtained exclusive cyclic polymer formation at a 1:1 reaction stoichiometry.[83] Deviation from a 1:1 stoichiometry resulted in substantial molecular weight loss, as expected for a step-growth polycondensation.[24, 25]

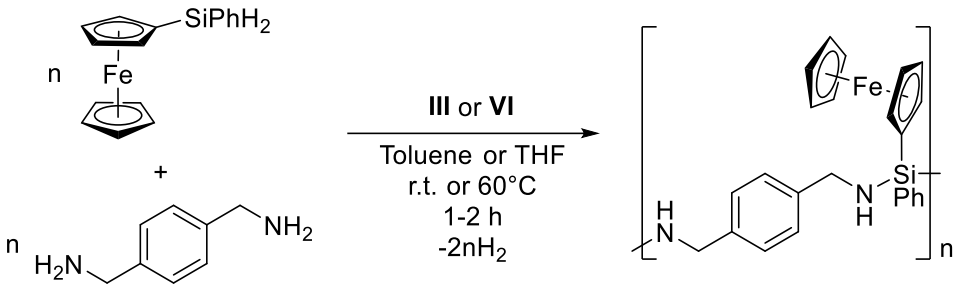

Scheme 5: Synthesis of polymers **P1-P6**.

Hydrolytically sensitive backbone Si-N bonds result in vulnerability towards hydrolysis and as a result, analysis by gel permeation chromatography was inappropriate. We, therefore, turned to diffusion ordered NMR spectroscopy (DOSY) to provide an alternative method for molecular weight determination. Using monodisperse polystyrene standards and a protocol described by Grubbs *et.al.*,[87] diffusion coefficients were correlated to estimated molecular weights, providing values broadly in agreement with end group analysis (Table 1).

Although the catalyst loading could be lowered to 3.3 mol% without any significant reduction in M_n (Table 1, **P2**), further reduction to 1 mol% resulted in oligomeric species (Table 1, **P3**) terminated by both NH- and SiH- chain ends. Replacement of the catalyst **III** with the analogous homoleptic alkyl, $Ba(CH(SiMe_3)_2)_2.(THF)_2$ (**VI**), did not significantly impact upon molecular weight (Table 1, **P4**). Reactions carried out in THF allowed the use of higher monomer concentrations, but did not exert a significant influence on the estimated molecular weight (Table 1 **P5**). Although dehydrocoupling proceeded efficiently at room temperature (Table 1 **P6**), the reactions were typically carried out at 60°C to ensure complete conversion and to shorten reaction times. The addition of fresh catalyst upon complete conversion did not result in any significant alternation in molecular weight, indicating that the reaction was not limited by catalyst deactivation (Table 1, **P7a** and **P7b**).

Table 1: Ba-catalyzed dehydropolymerisation of **1** and *p*-xylylenediamine. [a] Number average molecular weight calculated from ^{1}H NMR end-group analysis. [b] Degree of polymerization calculated from ^{1}H NMR end-group analysis. [c] Number average molecular weight estimated by ^{1}H DOSY NMR spectroscopy. * Product obtained following addition of a further 5 mol% **III** to the reaction mixture after two hours.

Polymer	Catalyst	Ratio Si:N:Ba	Solvent (concentration/M)	Temperature/°C (time/hours)	$M_{n,\,end\ group}$ / (g mol^{-1})[a]	$X_{n,\,end\ group}$[b]	$M_{n,\,DOSY}$ / (g mol^{-1})[c]
P1	**III**	20:40:1	Toluene (0.48)	60 (2)	9800	22.7	12,600
P2	**III**	30:60:1	Toluene (0.48)	60 (2)	9000	20.9	11,600
P3	**III**	100:200:1	Toluene (0.48)	60 (2)	1800	4.0	1,700
P4	**VI**	30:60:1	Toluene (0.48)	60 (2)	11000	25.6	11,900
P5	**III**	30:60:1	THF (1.33)	25 (1)	9300	21.7	12,200
P6	**III**	30:60:1	Toluene (0.46)	25 (3)	17400	41.0	21,700
P7a	**III**	30:60:1	Toluene (0.46)	25 (3)	12400	29.2	12,200
P7b	**III**	25:50:2*	Toluene (0.46)	25 (5)	10500	24.7	14,300

Synthesis of 3 and subsequent reactions with benzyl amine. Of potentially greater interest than pendant ferrocene-containing polymers are polymers where the ferrocene group forms part of the main chain. With this in mind, the bifunctional hydrosilane **3** was synthesised and its dehydrocoupling reactivity with benzyl amine was investigated. Expecting mono-substitution at each silicon atom, compound **3** was coupled to two equivalents of benzyl amine in the presence of 10 mol% **III** (Scheme 6). Although all the starting material had been consumed after 16 hours at 60°C, the resultant ^{1}H NMR spectrum was complex and indicative of the formation of several compounds. Consistent with this apparent poor stoichiometric control, cooling a hexane/toluene solution of the crude product to –30°C resulted in the isolation of orange crystalline blocks, which were shown by single crystal X-ray diffraction analysis to be the tetra-substituted product **4** (Figure 2). Compound **4** displays similar structural parameters to compound **2** and crystallizes in the triclinic space group *P-1*, with an asymmetric unit comprising half a molecule in which the iron centre is coincident with a crystallographic inversion centre.

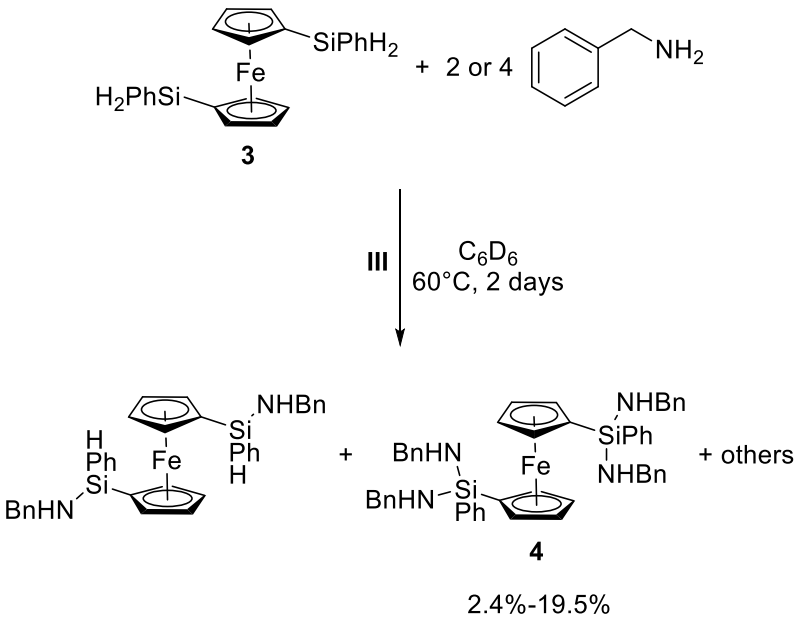

Scheme 6: The Ba-catalyzed dehydrocoupling of compound **3** with two equivalents of benzyl amine to yield compound **4**.

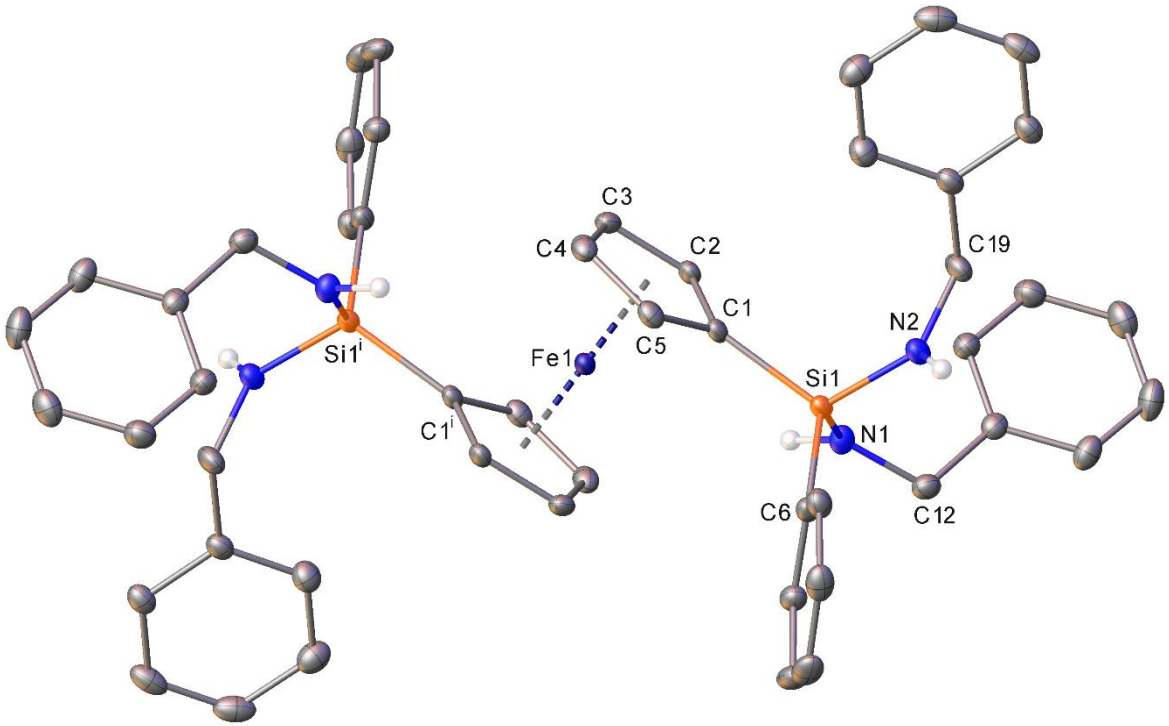

Figure 2: ORTEP representation of the X-ray crystal structure of **4**. Thermal ellipsoids are shown at the 30% probability level. Hydrogen atoms are omitted for clarity, except for those bound to nitrogen. Labels superscripted with 'i' are related to those in the asymmetric unit by the *–x*, 1 – *y*, 1 – *z* symmetry operation.

Synthesis of polycarbosilazanes with ferrocene in the main polymer chain. The catalytic dehydrocoupling of **3** and 1,4-$(H_2NCH_2)_2C_6H_4$ was undertaken. After stirring overnight at 60°C to ensure complete conversion, the reaction was quenched by addition of non-dried hexane,

and an orange solid (**P8**) was obtained on removal of solvent (Scheme 7). The ^{1}H NMR spectrum of **P8** comprised numerous overlapping signals that precluded detailed assignment. The observation of multiple Si-H environments, however, was indicative of several different repeat units and consistent with the isolation of the molecular compound (**4**), a likely result of extensive branching and cross-linking to form a network-type structure.

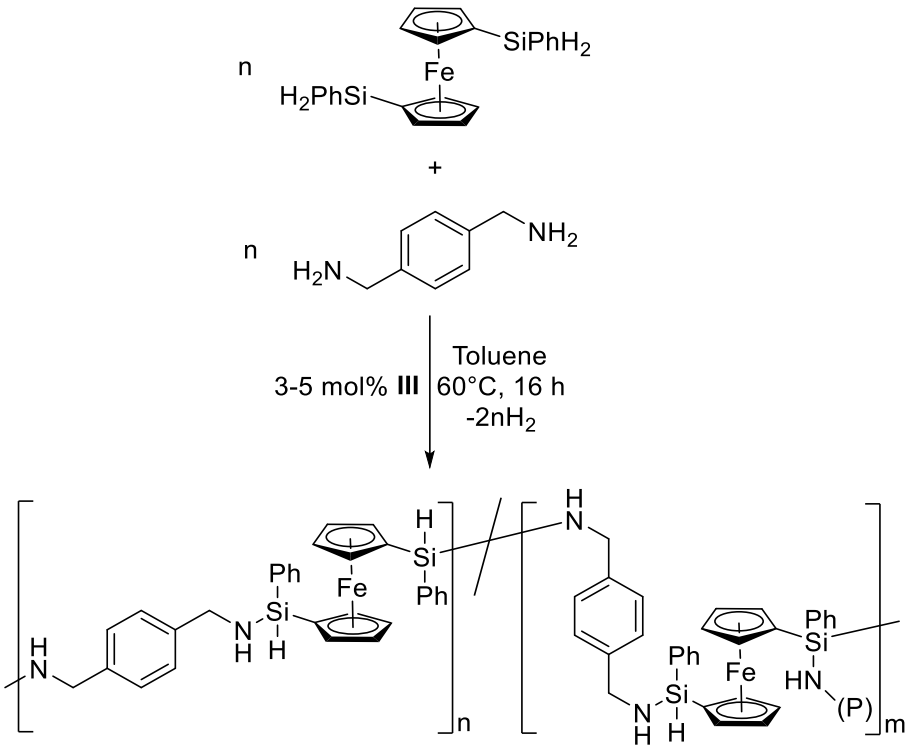

Scheme 7: Synthesis of polymers **P8-P10**. Note that the shown structure of the polymer is simplified. In reality, numerous repeat units are possible depending on the extent of substitution at Si, some of which may give rise to oligomeric or polymeric side chains, which are shown is this scheme as '(P)'.

Polymerization of **3** and 1,4-$(H_2NCH_2)_2C_6H_4$ was repeated but with isolation of the product by precipitation. DOSY experiments gave very high diffusion coefficients and an estimated molecular weight of 19,000-28,000 Da (Table 2). Molecular weights estimated from DOSY experiments should be treated with particular caution for these samples, however, given that any branched or network-type structure is likely to possess a very different hydrodynamic radius compared to the polystyrene standards used for calibration. When the catalyst loading was reduced from 5 mol% to 3.3 mol%, a lower molecular weight was obtained, while attempted reaction was attempted with 1 mol% **III** resulted in incomplete conversion and the isolation of oligomeric species and starting material. Whilst polymers **P8-P10** are interesting materials, their poorly defined nature rendered detailed characterization and rational synthesis challenging. This prompted a change in methodology for the synthesis of well-defined poly(carbosilazane)s with ferrocene in the main polymer chain.

Table 2: Dehydropolymerization of **3** and *p*-xylylenediamine catalyzed by compound **III**. Reactions were performed in toluene at 60°C for 2 hours, except for **P8**, where polymerization was carried out at 60°C for 16 hours. [a] Number average molecular weight estimated by ^{1}H DOSY NMR spectroscopy. *DOSY of **P9** displayed two different diffusion coefficients.

Polymer	Ratio Si:N:Ba	Concentration / M	$M_{n,\ DOSY}$ / (g mol^{-1}) [a]
P8	40:40:1	0.10	3600
P9	40:40:1	0.39	19200, 27800*
P10	60:60:1	0.39	5200

The catalytic dehydrocoupling of 1,1'-bis(amino)ferrocene (**VII**) with diphenylsilane was also investigated. Rather than the generation of polymer, however, NMR spectroscopy revealed almost complete selectivity towards the formation of cyclic silazane[3]ferrocenophane **5** (Scheme 8), whose structure was confirmed by single crystal X-ray diffraction analysis (Figure 3). When two equivalents of diphenylsilane were used, **5** persisted as the major product in 70% spectroscopic yield with the remaining products assumed to be linear species, which eluded unambiguous characterization. Although there are several examples of metallocenophanes with nitrogen-containing *ansa*-bridges (excepting ferrocene-based N-heterocyclic carbenes and numerous examples where the 1,1'-bisamino- amido- and imido-ferrocene moiety has been used as a chelating ligand),[88-102] compound **5** is of particular interest since it is, to the best of our knowledge, the first example with a N-Si-N bridging unit.

Intrigued by the possibility of using Ae-catalyzed dehydrocoupling as a tool for the synthesis of interesting new metallocenophanes, a similar reaction was carried out using (phenylsilyl)ruthenocene **6** in the place of diphenylsilane. As expected, a single equivalent of compound **6** reacted rapidly with 1,1'-bis(amino)ferrocene in the presence of 5 mol% barium-amide **III** to provide a single product, which prevails even when an excess of **6** is present. Although the ^{1}H NMR spectrum was complex, this may be ascribed of a resultant diastereotopicity at the silicon centre and is consistent with formation of the heterobimetallic silazane[3]ferrocenophane (**7**), whose structure was confirmed by single crystal X-ray diffraction (Figure 4). Although release of ring strain typically provides a thermodynamic driving force in the ring opening polymerisation of metallocenophanes,[103-106] inspection of the crystal structures of compounds **5** and **7**, suggest that they are relatively un-strained molecules due to limited ring tilt (a deviation of Cp-Fe-Cp linearity) or geometrical distortion in the *ansa*-bridge (Table 3). Whilst ring-tilt (or lack thereof) is not necessarily indicative of strain,[103-106] a preliminary investigation of **5** and **7** by differential scanning calorimetry (DSC) did not reveal evidence of any thermal ROP process (see figures S24 and S25 in the Supplementary Information).

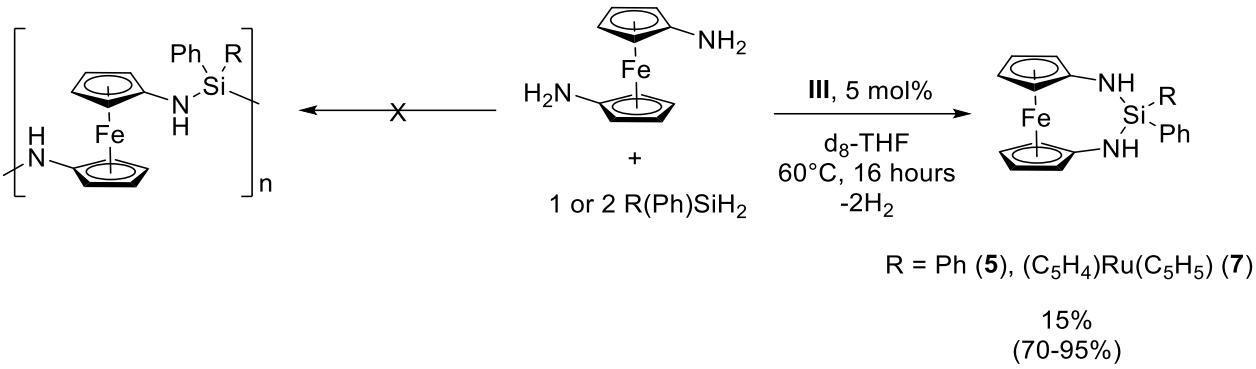

Scheme 8: Barium-catalyzed dehydrocoupling of 1,1'-bis(amino)ferrocene and dihydrosilanes to yield **5** and **7**. Values in parentheses refer to the spectroscopic yield determined from ^{1}H NMR of the crude product.

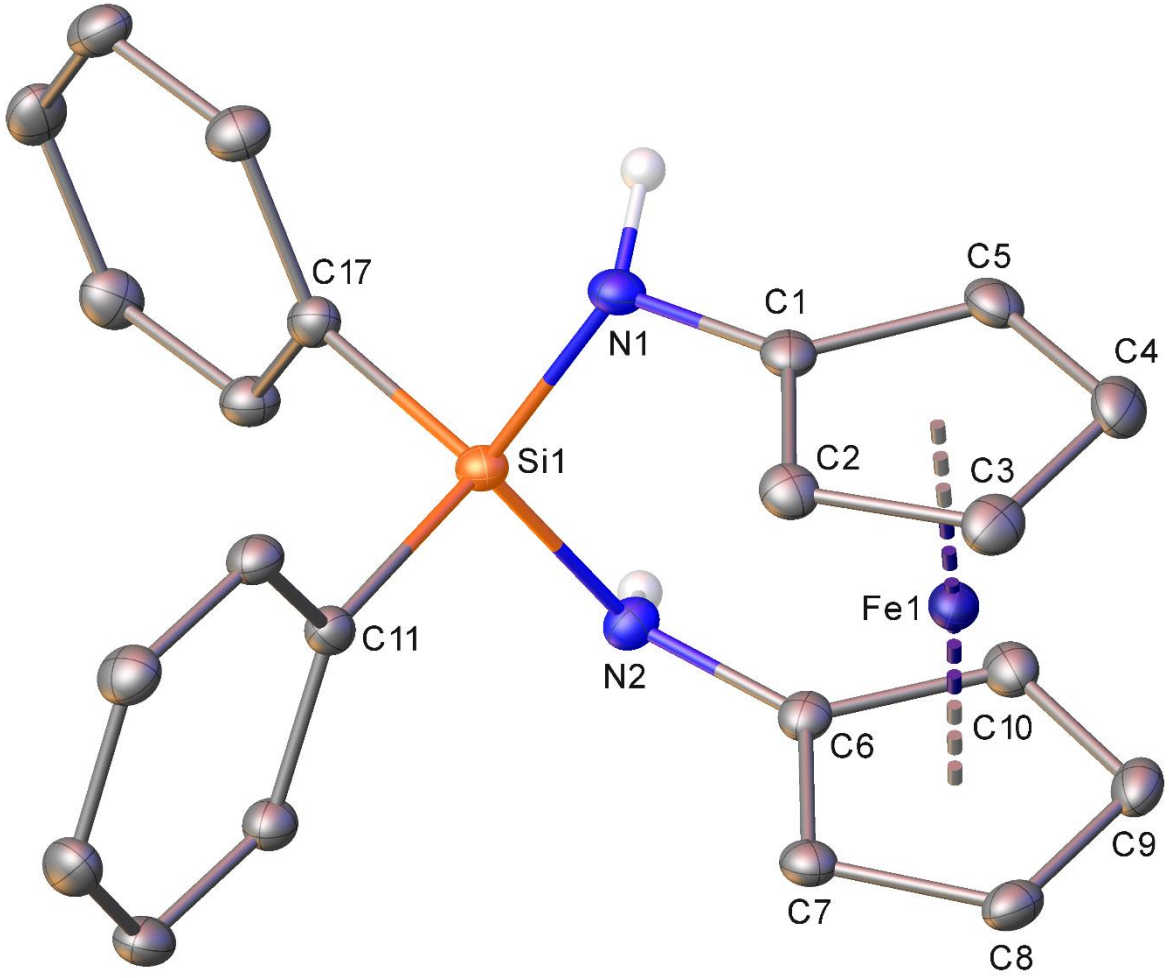

Figure 3: ORTEP representation of the X-ray crystal structure of **5**. Thermal ellipsoids are shown at the 30% probability level. Hydrogen atoms are omitted for clarity, except for those bound to nitrogen.

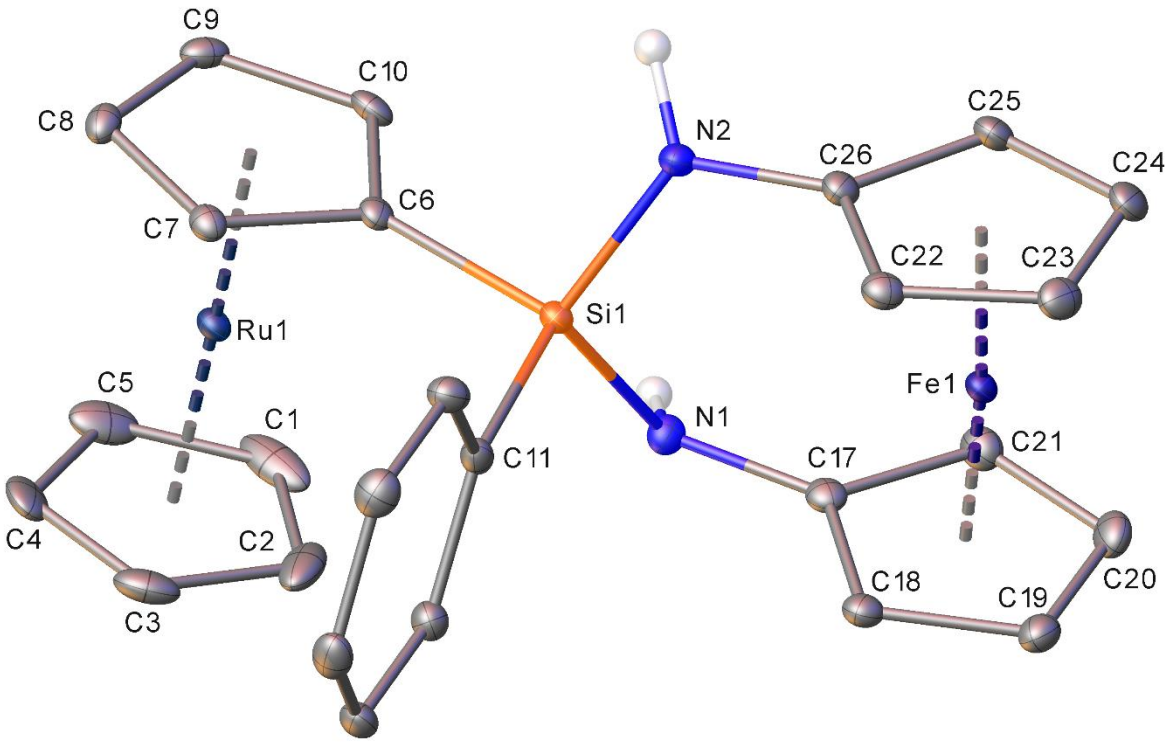

Figure 4: X-ray crystal structure of **7**. Thermal ellipsoids are shown at 30% probability level. Hydrogen atoms are omitted for clarity, except for those bound to nitrogen.

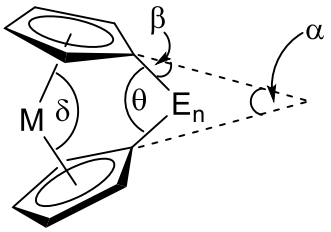

Figure 5: Depiction of geometric parameters α, β, δ, and θ in [n]metallocenophanes.

Table 3: Geometric analysis for compounds **5** and **7**.

Compound	**α/°**	**β/°**	**δ/°**	**θ/°**
5	4.61	3.37	175.51	11.14
7	6.30	3.62	174.41	12.09

After failing to obtain polymer from 1,1'-bis(amino)ferrocene, we returned to compound **3**, this time in partnership with the secondary bifunctional amine, *N*,*N*'-dimethyl-*p*-xylylenediamine, 1,4-(H(Me)NCH$_2$)C$_6$H$_4$. We surmised that the secondary amine would impose an enhanced level of steric control, disfavouring multiple substitution at silicon, and favouring linear polymer. Although *N*,*N*'-dimethyl-*p*-xylylenediamine has also previously been investigated as a

monomer by Bellini *et.al.*, for similar reasons they found that the polymer chain was unable to propagate beyond molecular species (**VIII**, Scheme 9), presumably due to steric hindrance at the newly formed silazane.[84]

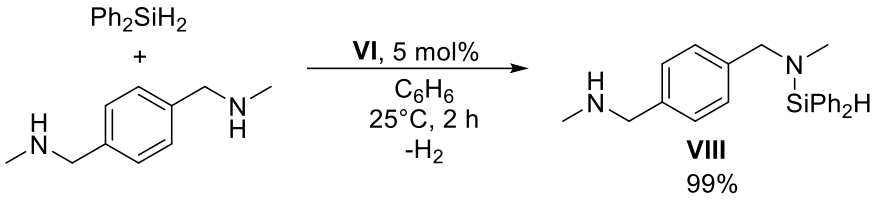

Scheme 9: The barium-catalyzed dehydrocoupling of diphenylsilane and *N,N*'-dimethyl-*p*-xylylenediamine to yield compound **VIII**, reported by Sarazin and co-workers.[84]

We attempted the same reaction, using two equivalents of diphenylsilane, finding that substitution at both ends of the bifunctional amine could occur and resulting in isolation of compound **8** (Scheme 10), which crystallized from a saturated toluene solution on cooling to −30 °C (see supplementary information Figure S4 for crystal structure).

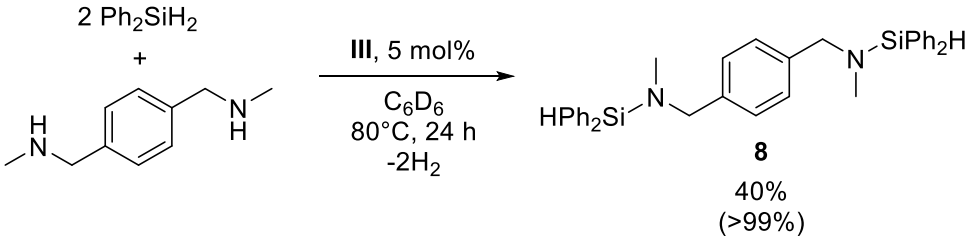

Scheme 10: The barium-catalyzed dehydrocoupling of two equivalents of diphenylsilane and 1,4-$(H(Me)NCH_2)_2C_6H_4$ to yield compound **8**.

These results suggest that copolymerisation of **3** with 1,4-$(H(Me)NCH_2)_2C_6H_4$ could result in the selective formation of a linear polymer with a well-defined repeat unit through controlled dehydrocoupling of one Si-H bond per nitrogen centre. Indeed, when dehydrocoupling of **3** and 1,4-$(H(Me)NCH_2)_2C_6H_4$ was attempted in a 1:1 stoichiometric ratio with **III**, an orange solid (**P11**) was obtained following precipitation into pentane at −78°C (Scheme 11). Analysis by ^{1}H DOSY NMR revealed a diffusion coefficient of 1.24×10^{-6} cm^2s^{-1}, giving an estimated M_n of ~10300 Da (Table 4). The product provided a clean ^{1}H NMR spectrum, with clearly distinguished peaks corresponding to mid-chain SiH and end-chain SiH_2 groups, whereas no evidence for amine terminated polymer chains could be observed. Although integration of the SiH peaks allowed a degree of polymerisation to be estimated, the M_n calculated by end-group analysis was substantially lower than that estimated from DOSY, possibly a result of the sterically hindered chain giving rise to low flexibility and a relatively large hydrodynamic radius (compared to polystyrene of a similar molecular weight, or other polymers described herein).

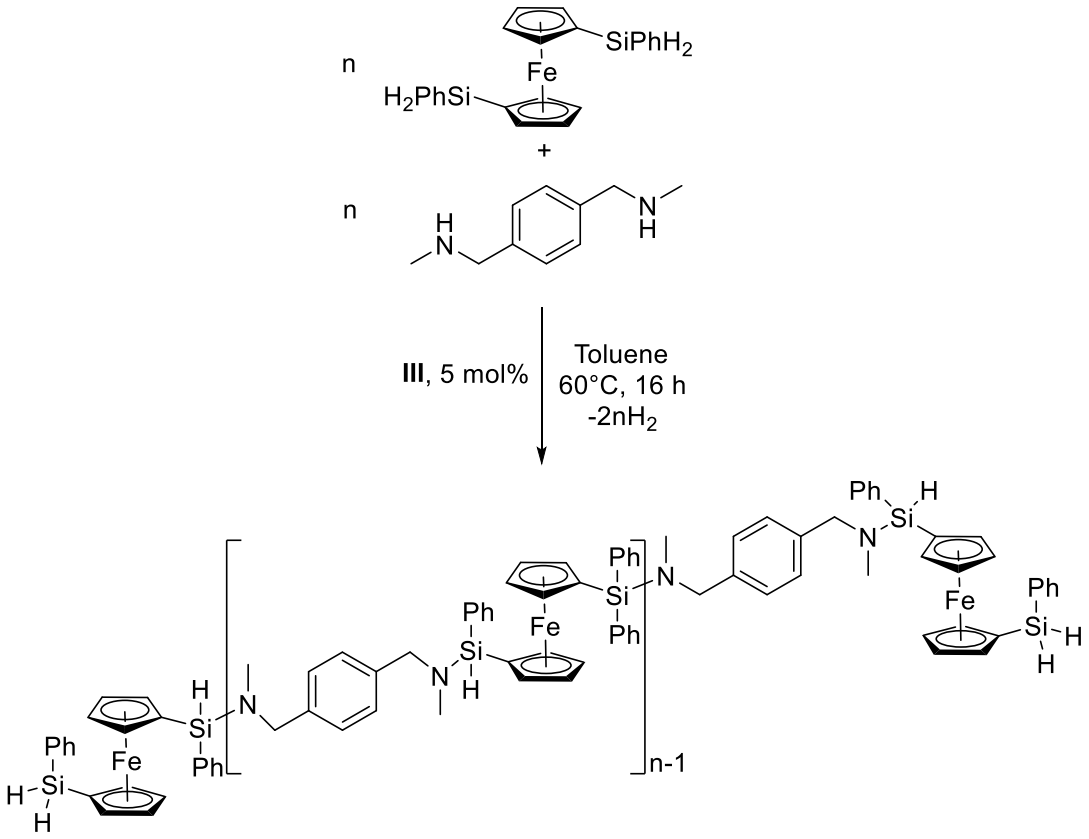

Scheme 11: Synthesis of polymer **P11** *via* the barium-catalyzed dehydrocoupling of **3** and *N,N*'-dimethyl-*p*-xylylenediamine.

A higher molecular weight product could be obtained using a higher concentration and lower temperature (Table 4, **P12**). In this case, whereas ^{1}H NMR spectroscopy provided no evidence of terminal silane groups, some terminal amine groups could be detected, to provide a number average molecular weight of ~17,000 Da on integration (assuming an absence of cyclic products) and in good agreement with that obtained by DOSY NMR spectroscopy.

Amines have not commonly been observed to dehydrocouple with two equivalents of tertiary silane under Ae-catalysis,[82, 85] and, with only one Si-H bond available per silicon atom, the use of a bifunctional tertiary silane was expected to yield well-defined linear polymer. To this end, the dehydropolymerisation 1,1'-bis(dimethylsilyl)ferrocene (**IX**) [107, 108] and 1,4-$(H_2NCH_2)_2C_6H_4$ was carried out in the presence of 3.3 mol% **III** (Scheme 12). Following precipitation into hexane at −78°C, a gummy solid was obtained (**P13**). The product was analysed by ^{1}H NMR spectroscopy to provide a simple spectrum without Si-H resonances. A clear triplet at 3.62 ppm was assigned to chain-end methylene groups allowing a molecular weight of $M_n \approx$ 6500 Da to be estimated. Furthermore, DOSY NMR spectroscopy yielded a diffusion coefficient of 1.71×10^{-6} cm^2s^{-1}, corresponding to an estimated M_n of ~5500 Da, in reasonable agreement with end-group analysis.

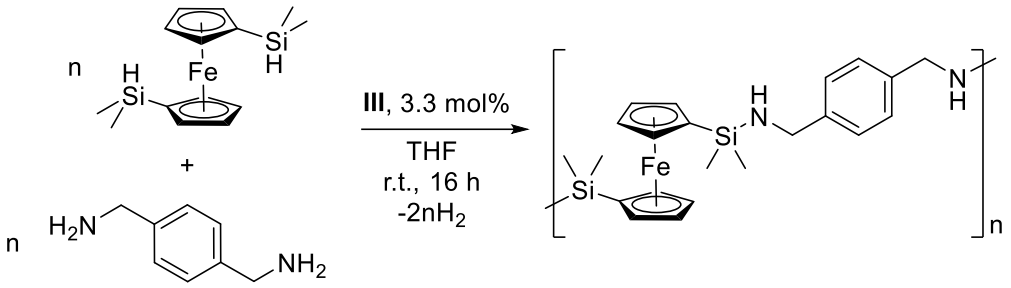

Scheme 12: Synthesis of polymer **P13**.

Table 4: Ba-catalyzed dehydropolymerisation of compounds **3** or **IX**, with *N*,*N*'-dimethyl-*p*-xylylenediamine or *p*-xylylenediamine, respectively. Each reaction was stirred for 16 hours to ensure complete conversion. [a] Number average molecular weight calculated from ^{1}H NMR end-group analysis. [b] Degree of polymerisation calculated from ^{1}H NMR end-group analysis. [c] Number average molecular weight estimated by ^{1}H DOSY NMR spectroscopy.

Polymer	Silane	Amine	Ratio Si:N:Ba	Solvent (concentration / M)	Temperature / °C	$M_{n,\,end\ group}$ / (gmol^{-1})[a]	$X_{n,\,end\ group}$[b]	$M_{n,\,DOSY}$ / (gmol^{-1})[c]
P11	**3**	1,4-(H(Me)N CH_2)$_2$$C_6H_4$	40:40:1	0.06	60	5300	8	10300
P12	**3**	1,4-(H(Me)N CH_2)$_2$$C_6H_4$	40:40:1	0.46	25	16900	30	17600
P13	**IX**	1,4-(H_2NCH_2)$_2$$C_6H_4$	60:60:1	0.74	25	6500	10	5500

Electrochemical studies. Ferrocene-containing polymers often present interesting electrochemical properties due to the presence of multiple redox-active sites.[20, 109, 110] Using cyclic voltammetry, a brief and qualitative investigation was undertaken into the electrochemistry of the ferrocene-containing polycarbosilazanes. Polymer **P1** displays a well-defined and fully reversible single electron redox process, corresponding to the Fe^{3+}/Fe^{2+} redox couple, with $E_{1/2}$ lying very close to that of the reference ferrocene redox system (Figure 6). In comparison to the silane monomer **1**, $E_{1/2}$ occurs at slightly lower potentials, possibly reflective of increased electron density at iron. The decrease in peak current for **P1** relative to that of **1** may be rationalized by recourse to the Randles-Sevcik equation (Eq. 1), which accounts for the contributions of the diffusion coefficient, *D*, and the number of electrons transferred per molecule diffusing to the electrode, *n*.[111]

$$I_{peak} = 0.446\, n^{3/2} D^{1/2} F^{3/2} \mathrm{Ac} \sqrt{\frac{v}{RT}} \qquad (1)$$

Inspection of Eq. 1 reveals that the peak current is dependent on *n*, *D*, the Faraday constant *F*, the area *A*, the concentration *c*, the scan rate *v*, the gas constant *R* and the absolute temperature *T*. If fast electron transfer is assumed, an increase in current with square root of

scan rate may be predicted for **P1**, **1**, and **2** (see supporting information). For the polymer, *n* becomes the degree of polymerization to reflect the number of ferrocene units, *D* decreases by a factor $(molecular\ volume)^{-0.6}$,[112] and *c* decreases by a factor of 1/(degree of polymerisation). Taking the molecular volume as proportional to the degree of polymerisation, therefore, these factors provide almost perfect mutual compensation to predict a very similar peak current for both monomer and polymer. Although polymer **P1** displays an almost identical peak current when compared to the model carbosilazane, compound **2**, the peak shape for the polymer oxidation is substantially altered. As well as a smaller peak separation (Δ*E*), typical for a multiple-electron transfer process,[113] **P1** displays a distinctly sharp reduction peak. This is likely to be due, at least in part, to some adsorption and accumulation of the multiply oxidised polymer onto the electrode surface. Although the peak-to-peak separation for an ideal multi-electron transfer should be $\Delta E_{peak} = 2.218\ \frac{RT}{nF}$,[111] ideal conditions are unlikely for these polymer systems.

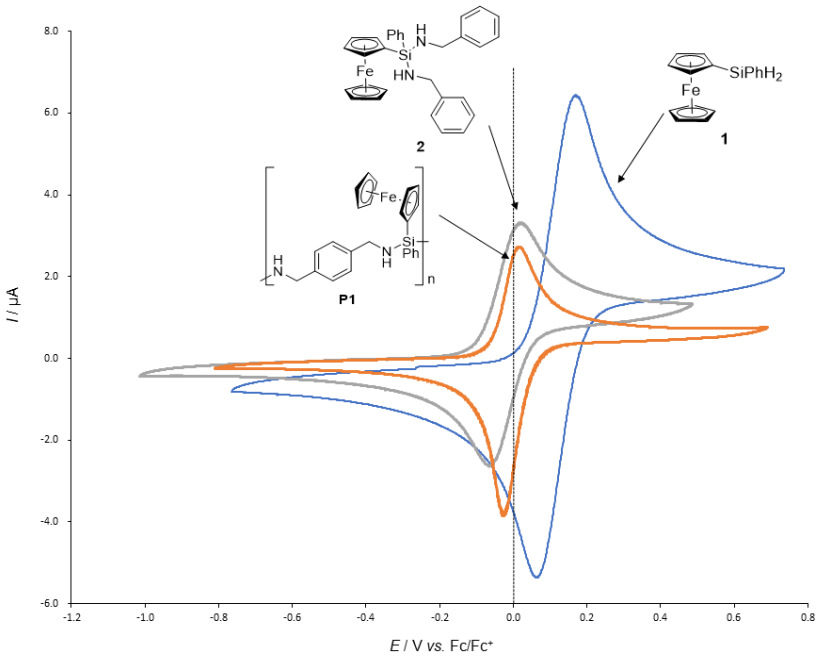

Figure 6: Cyclic voltammogram of polymer **P1**, compared to compounds **1**, and **2**. In each case solution concentrations are ca. 1 mM in molecular or monomer concentration obtained with a 1 mm diameter platinum disc electrode immersed in dichloroethane containing 0.1 M NBu_4PF_6 with at a scan rate of 100 mVs^{-1}.

Cyclic voltammograms for the main-chain ferrocene containing polymer, **P8**, displayed the most positive $E_{1/2}$ (see Table 5). Similar structures (based on the same monomer units) such as **P9** and **P10** showed some variation in the midpoint potential (and some peak broadening), possibly due to effects of branching in the polymer structure. In contrast, monomer **5** exhibited

the most negative $E_{1/2}$, most likely due to presence of two silazane substituents (c.f. compound **2** in Figure 1 with a single silazane substituent).

The linear *N*-methylated polymer **P11** displayed a single redox peak without significant broadening, but with the lowest current response compared to the other polymer systems. This could be linked to the relatively high M_n (~10000 Da), and resultant slower diffusion. Although **P1** also exhibited a relatively high M_n (~12600 Da), the ferrocene units are pendant to the polymer chain and thus more accessible to the electrode, resulting in a higher current. In contrast to the phenyl-substituted derivatives, the dimethylsilyl-substituted polymer **P13** displayed a reversible multi-electron redox event and yielded a significantly higher peak current (see supplementary information, Figure S202), in this case probably linked to a lower M_n (~5500 Da). **P13** also displayed a shift of $E_{1/2}$ towards higher potentials relative to the hydrosilane monomer **IX**. This is likely to be the result of the contrasting electronic natures of the electron donating dimethylsilyl and electron withdrawing phenylsilyl substituents. Furthermore, for **P13** the symmetrical peak shape upon both oxidation and reduction may be indicative of the polymer remaining in solution and more limited adsorption of the charged polymer to the electrode surface.

Table 5: Cyclic voltammetry data for samples dissolved in ca. 1 mM molecular/monomer concentration obtained at a 1 mm diameter platinum disc electrode immersed in dichloroethane containing 0.1 M NBu_4PF_6 at 100 mV/s. Potentials are referenced to ferrocene/ferrocenium.

Compound	Concentration [a]	$E_{1/2}$ / V [b]	ΔE_{peak} / mV	$I_{peak, ox}$ / µA	$I_{peak, red}$ / µA
P1	1 mM	0.001	41	2.45	-3.87
1	1 mM	0.115	100	5.44	-5.78
2	1 mM	-0.016	90	3.40	-3.49
P8 [c]	1 mM	0.135	81	2.07	-1.98
P9	1 mM	0.078	108	2.34	-2.54
P10	1 mM	0.098	207	2.52	-2.11
P11	1 mM	0.065	87	1.52	-1.64
3	1 mM	0.115	95	3.73	-3.99
4	0.4 mM	0.128	100	1.26	-1.39
P13	1 mM	0.171	85	2.33	-3.29
IX	1 mM	0.119	74	2.53	-2.65

[a] *approximate concentration of molecular systems or of monomer in polymer systems*

[b] *the midpoint potential is defined here as* $E_{1/2} = ½(E_{p,ox} + E_{p,red})$

[c] *a shoulder peak occurs at* $E_{1/2}$ *= -0.02 V vs. Fc/Fc+ possibly due to oligomer impurities or due to adsorption*

Thermogravimetric analysis. Polycarbosilanes, polysilazanes, and polycarbosilazanes are well known for their utility as precursors to SiC, Si_3N_4, and Si/C/N ceramics.[58, 60-63]

Furthermore, some ferrocene-containing polymers have proven themselves as excellent precursors to magnetic ceramic materials.[114-121] In light of this precedent, ferrocene-containing polycarbosilazanes are attractive candidates as ceramic precursors.

To test their viability as ceramic precursors, the polymers were first analysed by thermogravimetric analysis (TGA). Samples were heated to 800 °C at 10°C/minute under a flow of N_2 (Figure 7). Each of the polymers synthesised in toluene displayed a minor weight loss below 200 °C, presumably resulting from evaporation of entrapped solvent. For this reason, ceramic yields discussed henceforth and displayed in Table 6 take the mass at 200 °C (at which temperature the material is considered solvent-free) to be 100%. **P1** displayed a ceramic yield of 43%: a relatively high value for a linear polymer. For comparison, linear polyferrocenylsilanes give ceramic yields in the range 17-58% at 600°C depending on the substituents at silicon.[114, 121] The relatively high ceramic yield obtained from **P1** is likely to be a result of cross-linking reactions during pyrolysis, which must necessarily proceed at a lower temperature, or a higher rate than competing depolymerization and loss of volatile fragments. Encouraged by the appreciable ceramic yield, and in the knowledge that ceramic yields can be substantially improved though utilisation of a crosslinked polymeric precursor, [117] a deliberately crosslinked polymer was synthesised by addition of phenylsilane to the reaction mixture after 45 minutes (by which point the reaction had stopped bubbling and was assumed complete). Notably, addition of phenylsilane was accompanied by immediate bubbling and a rapid increase in viscosity, before finally forming an immobile mass. Neither precipitation, nor solution phase characterisation were possible on account of insolubility, but an elastic orange solid (**P14**) was obtained following prolonged drying under vacuum. Thermogravimetric analysis of **P14** was carried out and it was found that even following vacuum treatment, polymer **P14** contains a large quantity (12 wt%) of entrapped solvent. Taking the solvent-free mass at 200 °C to equal 100% relative mass, therefore, **P14** displays a 12% improvement in ceramic yield compared to the non-crosslinked **P1** (Table 6). Although a compressed pellet of **P14** was also prepared and subjected to TGA, this pre-pyrolysis processing did not significantly influence the ceramic yield, and shape retention could not be achieved (Figure S6).

Polymer **P9** gave yet higher ceramic yields (61%). Although this result was initially ascribed to an already partially crosslinked polymer structure, TGA of the linear polymer **P11** presented the highest ceramic yield of all (64%). This emphasises that pre-crosslinked polymers are not a prerequisite for high ceramic yields and that the polycarbosilazanes which contain phenylsilyl groups are able to undergo cross-linking reactions during pyrolysis. In contrast, polymer **P13** (which contains dimethylsilyl groups) presented a very low ceramic yield (5.6%), suggesting

that a phenyl substituent and/or hydride at silicon are critical for the formation of ceramic material.

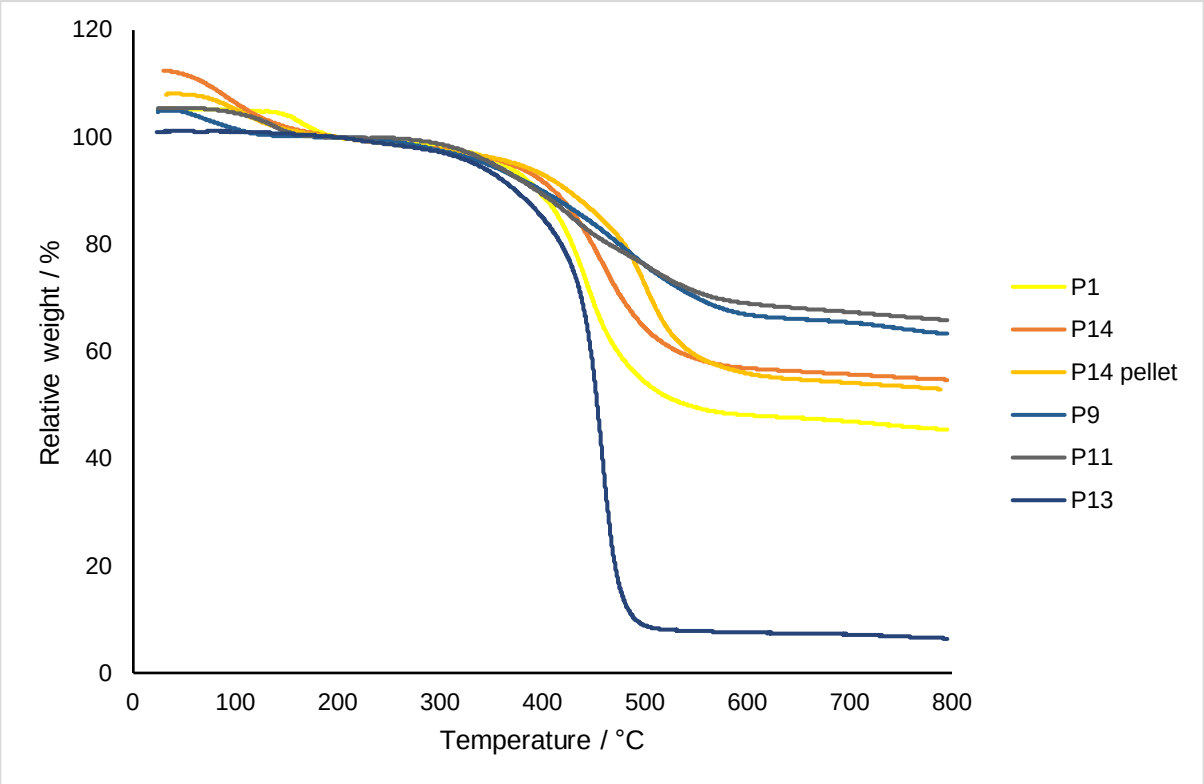

Figure 7: TGA traces of ferrocene-containing polycarbosilazanes, heated to 800°C at 10°C/min under a flow of N_2. To account for loss of entrapped solvent, the mass at 200°C is taken to equal 100%, subtracting the mass of solvent loss to result in starting relative weights greater than 100%. Uncorrected thermograms can be found in the supplementary information (Figure S23)

Table 6: Ceramic yields obtained after analysis of polymers by TGA at 10°C/min up to 800°C under a flow of N_2. Yields given are corrected for loss of entrapped solvent, with the mass at 200°C taken to equal 100%.

Sample	**Ceramic yield / %**
P1	43
P14	55
P9	61
P11	64
P13	6

Bulk polymer pyrolysis and ceramic characterization. Polymers **P5** and **P8** were subjected to pyrolysis on a larger scale in a tube furnace using the same heating protocol as for the TGA experiments. Ceramics **P5py** and **P8py** were obtained as charcoal-coloured powders.

Notably, both ceramics could be attracted towards a bar magnet, suggesting the presence of metallic iron or magnetite within the material.

Powder X-Ray diffraction (pXRD) was carried out, resulting in broad, low intensity diffraction patterns for both samples (Figure S8). Broad, weak maxima at 2θ = 44° (*d* = 2.05 Å) and 2θ = 63° (d = 1.43 Å), and a sharper peak at 2θ = 82° (*d* = 1.17 Å), however, were assigned to α-Fe,[122] while peaks at 2θ = 35° (*d* = 2.52 Å), 2θ = 72° (*d* = 1.31 Å), and 2θ = 83° (*d* = 1.16 Å) were assigned to hematite (α-Fe_2O_3).[123] This latter observation may be attributed to brief but unavoidable exposure of the samples to air on removal from the furnace. Although a broad peak at 2θ = 69° was also observed in both samples, the lack of other diagnostic peaks precludes its assignment. The low intensity of the diffraction pattern is attributed to the presence of small (i.e. nanoparticulate) crystalline α-Fe domains amongst an otherwise amorphous matrix. This is reminiscent of the ceramics obtained from the pyrolysis of polyferrocenylsilane (PFS) materials, where relatively low pyrolysis temperatures gave rise relatively low crystallinity nanoparticles.[114, 115, 117, 118] Although the resultant low reflection intensities and large line-widths also prevented meaningful Scherrer analysis on the reflections at low angle, an estimated crystallite size of 13 nm was obtained from the relatively intense peaks at 2θ = 82° and 2θ = 83°.

Scanning electron microscopy (SEM) (Figures S8 and S10) revealed an apparently non-porous structure for both samples, suggesting the likely melting and annealing of the polymer prior to pyrolysis. Energy dispersive X-ray spectroscopy (EDX) showed a homogeneous elemental composition, comprising predominantly of silicon, oxygen, and iron for **P5py** (Figure S10). **P8py** also showed significant quantities of barium (from residual catalyst), as well as sodium, sulfur, aluminium and chlorine contamination (Figure S11). By microtoming samples which had been finely ground and embedded in a resin, good quality Transmission Electron Microscopy (TEM) (Figure 8a, Figures S12-S14), and dark-field Scanning Transmission Electron Microscopy (STEM) images (Figures S15-S16) could be obtained. Analysis by this technique gave similar results for both samples and showed the presence of nanoparticles dispersed throughout a matrix of lower contrast (Figure 8a). In concordance with the pXRD data, the average nanoparticle size varied between 9 nm and 16 nm depending on the specific sample and region of study (Figures S12-S14). The elemental composition of the nanoparticles and surrounding matrix could also be mapped by EDX, confirming that iron was almost entirely concentrated in the nanoparticles whilst the surrounding ceramic was composed predominantly of silicon and carbon. A significant quantity of barium (from the polymerisation catalyst), oxygen (likely introduced during sample preparation), and nitrogen were also present (Figure 8b, Figures S17-S18).

a)

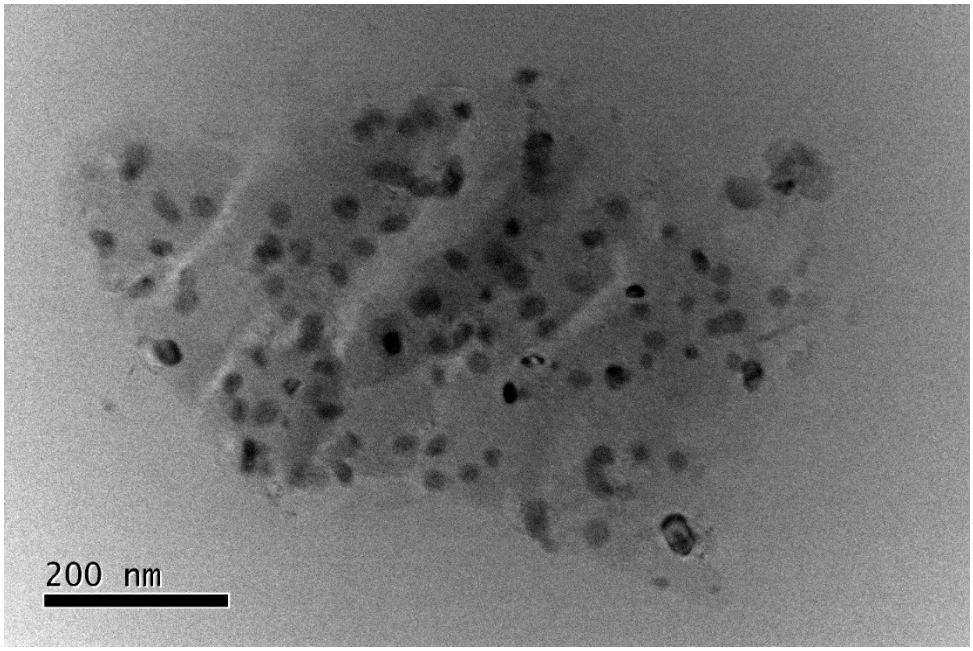

b)

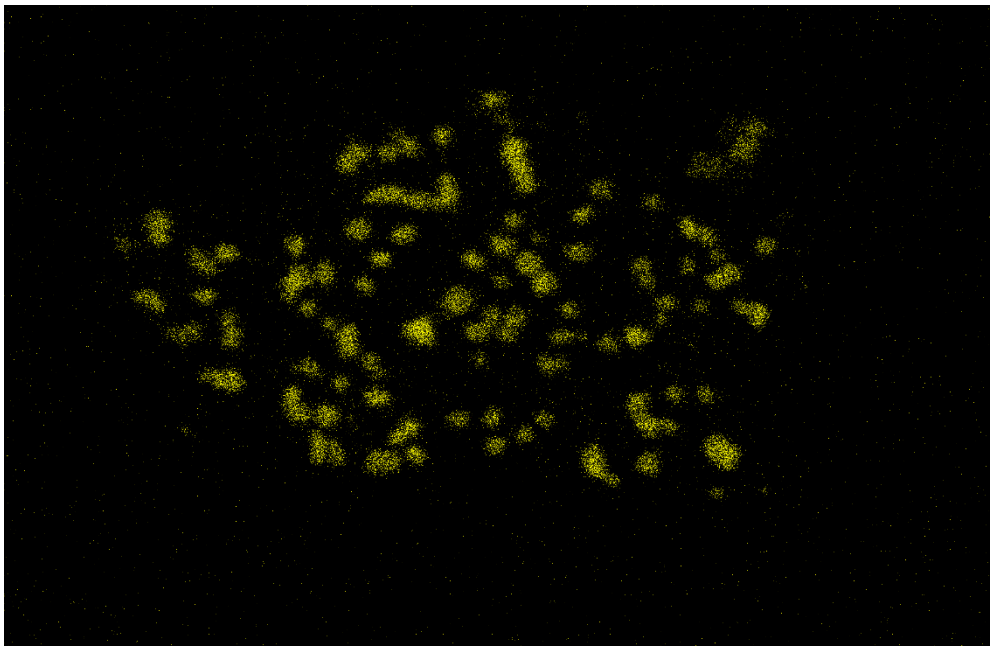

Figure 8: a) TEM micrograph and b) FeKα1 EDX map of **P5py**.

High resolution TEM (HRTEM) provided further evidence of the localised sample composition of the pyrolysed materials. Lattice fringes with a *d*-spacing of 0.217 nm observed in the nanoparticles were attributed to the (110) plane of α-Fe (Figure 9a, Figures S19-S20), an observation supported by Selected Area Electron Diffraction (SAED), which showed a predominantly polycrystalline diffraction pattern, with rings corresponding to the (110), and (211) lattice planes of α-Fe (Figure 9c, Figures S21-S22). The surrounding matrix was generally devoid of well resolved lattice fringes, however, some regions of graphitised carbon were visible (*d* = 0.365 nm, (002)) (Figure 9b, Figures S19b, S20b). Iron nanoparticles typically

display superparamagnetic behaviour (arising from single-domain particles) below a size of approximately 14 nm, above which they are ferromagnetic (i.e. multi-domain, capable of retaining magnetic hysteresis in the absence of an external magnetic field).[124] Hence, the magnetic characteristics of the nanoparticles present in samples **P5py** and **P8py** lie roughly on the border between superparamagnetism and ferromagnetism. Whilst the ceramic nanostructures in this study appear relatively unaffected by choice of polymer (i.e. main-chain or side chain ferrocene), previous studies on the pyrolysis of iron-containing polymers have displayed an ability to tune magnetic properties of the resulting ceramics through careful choice of pyrolysis conditions,[115] and similar future studies on the ferrocene-containing polycarbosilazanes described herein would be of interest.

a)

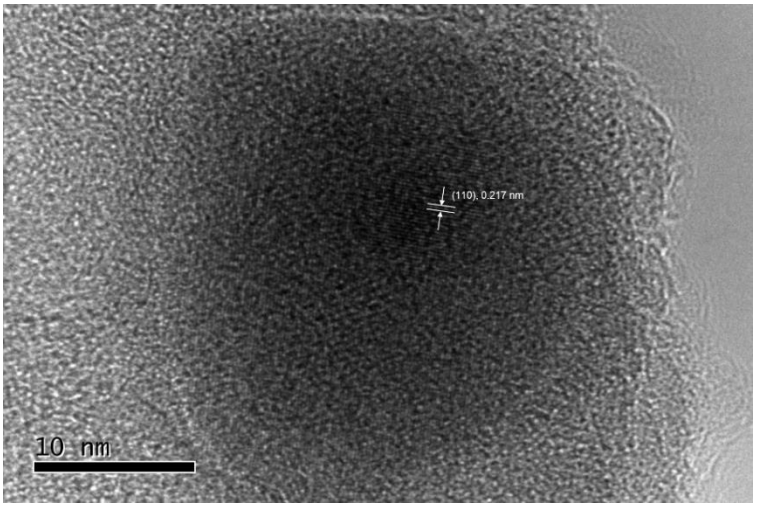

b)

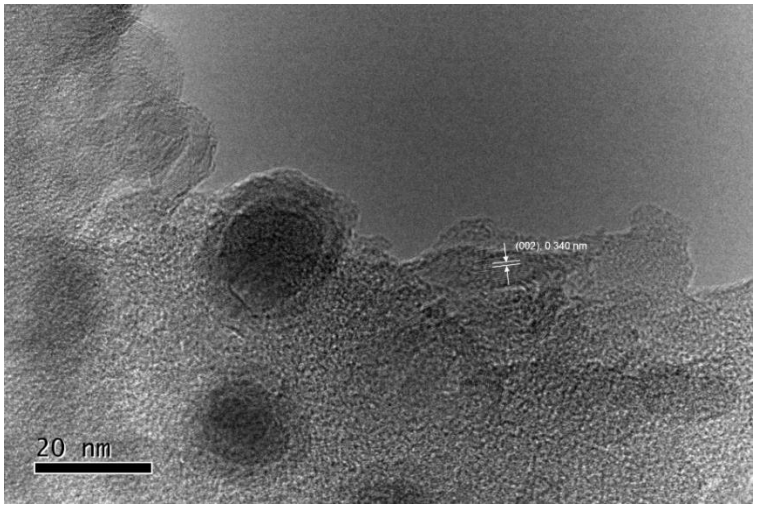

c)

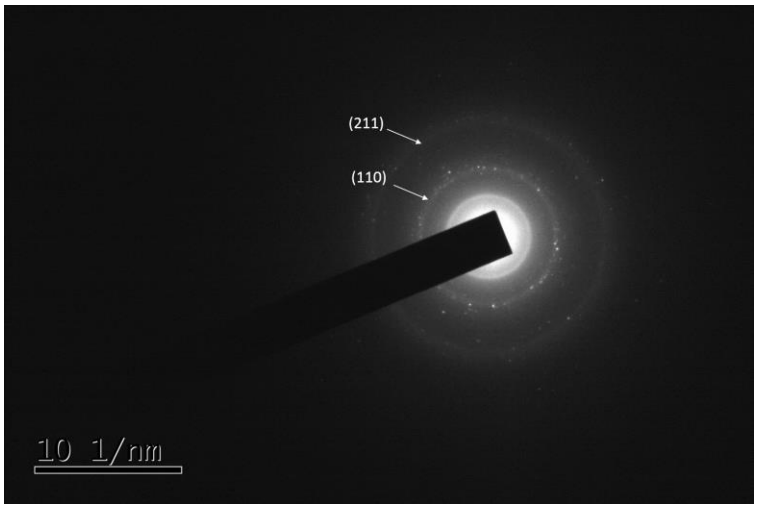

Figure 9: a) and b) HRTEM micrographs, and c) SAED diffraction pattern of **P8py**.

Conclusions.

In conclusion, the Ae-catalyzed dehydrocoupling of silanes and amines provides a useful synthetic route towards ferrocene-containing polycarbosilazanes. Through careful choice of monomer, well-defined linear polymers with pendant- or main chain-ferrocene units can be accessed. The facile and high yielding nature of the reaction allows estimated molecular weights of up to 20,000 Da to be achieved: a highly respectable figure for a step-growth polycondensation reaction, particularly one using 'inorganic' monomers. Novel silazane-bridged [3]ferrocenophanes could also be obtained in this way. Cyclic voltammetric analysis revealed that all polymers display a reversible single electron redox couple at the ferrocene moieties, which act as isolated redox centres. The described polymers serve as promising precursors to magnetic ceramic materials, with magnetic properties consistent with iron nanoparticles embedded within an amorphous silicon carbide/nitride matrix. Although further improvement of the ceramic yield could be obtained through the introduction of more tuneable crosslinking processes, highly respectable ceramic yields were achieved even with well-defined linear polymer. This latter feature is suggested to be a likely result of rapid crosslinking of the functionalized polymer backbone during pyrolysis. In summary, therefore, dehydrocoupling reactions of this type show great promise not only as a route to small molecules of novel structure but inorganic and functional organometallic polymers, presenting a relatively underexplored avenue towards new and interesting materials.

Experimental section

All reactions dealing with air and moisture-sensitive compounds were carried out under an argon atmosphere using standard Schlenk line and glovebox techniques in an MBraun Labmaster glovebox at O_2, H_2O < 0.1 ppm. NMR experiments using air-sensitive compounds were conducted in J. Young's tap NMR tubes prepared and sealed in a glovebox under argon. All NMR data were acquired at 298 K, on a Bruker 300 Ultrashield instrument for ^{1}H (300 MHz), Bruker 400 Ultrashield instrument for ^{1}H (400 MHz), and ^{29}Si (79.5 MHz), Bruker 500 Ultrashield instrument for ^{1}H (500 MHz) and ^{29}Si (99 MHz), and an Agilent ProPulse instrument for ^{1}H (500 MHz), ^{13}C (126 MHz) and ^{29}Si (99 MHz) spectra at 298 K. $^{1}H/^{13}C$ NMR spectra were referenced using residual solvent resonances and ^{29}Si NMR spectra were referenced using an external standard. Elemental microanalysis was carried out by Stephen Boyer of London Metropolitan University. Transmission electron microscopy and high-resolution transmission electron microscopy (HRTEM) was carried out on a JEOL1200EX II instrument. Scanning electron microscopy was carried out on a JEOL SEM 5600LV scanning electron microscope. Powder X-ray diffraction patterns were obtained on a Bruker D8 Advance diffractometer using Cu K_α radiation. Differential scanning calorimetry (DSC) was carried out

on a TA Instsruments DSC Q20. Samples were ramped from 0°C to 300°C at 10°C/min under an 18ml/min nitrogen flow. Hexane, Pentane, and Toluene for air- and moisture-sensitive reactions were provided by an MBraun Solvent Purification System and stored over 4Å molecular sieves. THF and Et_2O for use in air- and moisture-sensitive reactions were dried over sodium or potassium/benzophenone and distilled before use. Methanol was dried over activated 3Å molecular sieves. Anhydrous 1,2-dichloroethane was purchased from Sigma-Aldrich, and stored over activated 4Å molecular sieves. C_6D_6 was purchased from Sigma-Aldrich and dried over a potassium mirror prior to vacuum transfer into a sealed ampoule and storage in the glovebox under argon. Dry d_8-THF was purchased from Sigma Aldrich and used as received or purchased from Fluorochem and dried over 4Å molecular sieves followed by a potassium mirror, then vacuum transferred into a sealed ampoule and stored in the glovebox under argon. Terephthaldehyde was purchased from Sigma-Aldrich and further purified by sublimation. Ferrocene was purchased from Sigma-Aldrich or Avocado and purified by sublimation before use. Diphenylsilane and *N,N,N'N'*-tetramethylethylenediamine were purchased from Sigma-Aldrich and distilled from CaH_2. All other commercially available compounds were purchased from Sigma-Aldrich and used as received. *N,N*-dimethyl-*p*-xylylenediamine, [125] $[Ae(N(SiMe_3)_2)_2.(THF)_2]$ (Ae = Ca, Sr, Ba), [126-128] $[Ba(CH(SiMe_3)_2)_2.(THF)_2]$, [129] 1,1'-bis(amino)ferrocene,[130-132] and ruthenocene [133] were synthesised according to published procedures.

Diffusion ordered spectroscopy (DOSY) experiments. Diffusion Ordered Spectroscopy (DOSY) experiments were carried out on a Bruker 500 Ultrashield instrument. Samples were analysed at 1-2 mg/ml concentrations in C_6D_6. To avoid distorted diffusion coefficients, the spectra were collected without sample spinning. The Bruker dstebpgp3s convection corrected pulse sequence was used, with a diffusion delay of Δ = 60 ms and gradient pulse length of δ = 5 ms. Spectra were obtained over a 16 step gradient range from 10-90%. Spectra were processed using the MestReNova Bayesian DOSY transform function at a resolution factor of 0.1, 5 repetitions, and 512 points in the diffusion dimension over a range of ($1x10^{-7}$ – $1x10^{-4}$) cm^2s^{-1}. Molecular weights were estimated using a method described by Grubbs *et.al.*,[87] using six polystyrene standards of known molecular weight from 2000 to 30000 Da, purchased from Sigma-Aldrich. Plotting logD against $logM_n$ produced a linear calibration curve, to which all polymers were compared (Figure S26).

Cyclic voltammetry experiments. Cyclic voltammetry experiments were performed using an Ivium Technologies Compactstat potentiostat. Working, counter, and pseudo-reference electrodes were all platinum disks, 1 mm in diameter. Samples were prepared under a dry argon atmosphere in 1,2-dichloroethane (15 ml), at 1 mM concentration (molecular or

monomer concentration), except for compounds **4** (0.4 mM), **5** (0.6 mM), and **7** (0.4 mM). After measurements cobaltocenium hexafluorophosphate was added as an internal potential standard. The Cc/Cc^+ redox couple was found to occur at -1.39 V vs Fc/Fc^+, allowing comparison to the latter, more familiar internal reference system. Tetrabutylammonium hexafluorophosphate was used as the electrolyte at 0.1 M concentration.

Thermogravimetric analysis (TGA) and pyrolysis experiments. Thermogravimetric analysis (TGA) was carried out using a Universal Instruments TGA Q500. The temperature was ramped from room temperature to 800°C at 10°C/min under a 40 ml/min flow of nitrogen. Bulk pyrolysis experiments on **P5** and **P8** were carried under a flow of nitrogen, using the same heating protocol as for the TGA experiments, in a quartz tube furnace that was thoroughly purged with N_2 before the sample was loaded in a quartz boat. Following pyrolysis, the sample was cooled to ambient temperature under nitrogen before removal from the furnace. The pyrolysis products were stored in the glove box.

Synthesis of FeCp(CpSiPhH_2) (1). In the glove box, a Schlenk flask was charged with 4.0 g ferrocene (21.5 mmol) and 0.30 g KOtBu (2.7 mmol), which was then dissolved in approx. 50 ml THF. Another Schlenk flask was charged with 25.3 ml tBuLi (1.7 M in pentane, 43 mmol). The flasks were transferred to a Schlenk line, cooled to -78°C, and the tBuLi added dropwise to the ferrocene solution. The yellow suspension was stirred at -78°C for a further hour and 5.8 ml $SiPhH_2Cl$ (40 mmol) was added dropwise over 5 minutes. The reaction mixture was slowly warmed to ambient temperature, and stirred for a further 90 minutes. Volatiles were removed under reduced pressure, yielding a viscous orange slurry. The product was extracted with two portions of hexane followed by cannula filtration. Removal of the solvent yielded the crude product as a viscous orange oil. Prolonged sublimation at 70°C onto a cold finger and the walls of a Schlenk flask yielded the pure product as orange crystals suitable for single-crystal X-ray diffraction analysis, 3.4 g, 54% yield. ^{1}H NMR (300 MHz, C_6D_6) δ 7.69 – 7.58 (m, 2H, *o*-C_6H_5), 7.27 – 7.06 (m, 3H, *m,p*-C_6H_5), 5.14 (s, 2H, SiH_2), 4.17 (t, *J* = 1.6 Hz, 2H, 2,5-SiCp*H*), 4.13 (t, *J* = 1.8 Hz, 2H, 3,4-SiCp*H*), 3.98 (s, 5H, Cp*H*). ^{13}C NMR (126 MHz, C_6D_6) δ 135.58 (*o-Ph*), 133.47 (*i-Ph*), 129.92 (*m-Ph*), 128.37 (*p-Ph*), 75.08 (3,4-*Cp*Si), 72.16 (2,5-*Cp*Si), 69.04 (*Cp*), 61.15 (1-*Cp*Si). ^{29}Si NMR (99 MHz, C_6D_6) δ -35.81. Analysis calculated for $C_{16}H_{16}FeSi$: C 65.76, H 5.52, N 0%. Found: C 65.66, H 5.39, N 0%.

Reaction of benzyl amine with (phenylsilyl)ferrocene 1 to give FcSi(Ph)(HNBn)$_2$ 2. To a J. Youngs NMR tube was added 10 mg **2** ($3.42x10^{-5}$ mol), 7.48 µl benzyl amine ($6.84x10^{-5}$ mol), and 0.5 ml C_6D_6. 1 mg **I** ($2x10^{-6}$ mol) was dissolved in 0.1 ml C_6D_6 in a vial,

and added *via* pipette to the NMR tube resulting in immediate effervescence. On heating at 60°C for 16 hours, quantitative conversion to FcSi(Ph)(NHBn)$_2$ **2** was observed. Slow evaporation of a toluene solution yielded long, yellow crystalline needles, suitable for single crystal X-ray diffraction analysis. Yield 3.5 mg, 20.4%. Alternatively, compounds **II** or **III** could be used in the place of compound **I** at the same molar loading, reaching quantitative conversion to **2** after 20 minutes at room temperature followed by 1 hour at 60°C, or after 20 minutes at room temperature respectively. ^{1}H NMR (500 MHz, C_6D_6) δ 7.88 – 7.81 (m, 2H, *o*-Si*Ph*), 7.35 – 7.24 (m, 7H *o*-CH_2*Ph* + *m,p*-Si*Ph*), 7.23 – 7.18 (m, 4H, *m*-CH_2*Ph*), 7.14 – 7.07 (m, 2H, *p*-CH_2*Ph*), 4.20 (dd, *J* = 2.0, 1.4 Hz, 2H, 2,5-SiCp), 4.19 (dd, *J* = 2.0, 1.4 Hz, 2H, 3,4-SiCp), 4.13 (d, *J* = 2.5 Hz, 2H, NHCH_2), 4.12 (d, *J* = 2.1 Hz, 2H, NHCH_2), 3.93 (s, 5H, Cp), 1.43 (t, *J* = 8.0 Hz, 2H, N*H*). ^{13}C NMR (126 MHz, C_6D_6) δ 144.52 (*i*-Si*Ph*), 137.98 (*i*-CH_2*Ph*), 135.02 (*o*-Si*Ph*), 129.75 (*o*-CH_2*Ph*), 128.65 (*m*-CH_2*Ph*), 128.11 (*p*-Si*Ph*), 127.36 (*m*-Si*Ph*), 126.79 (*p*-CH_2*Ph*), 74.30 (2,5-Cp), 71.36 (3,4-Cp), 68.86 (Cp), 46.07 (CH_2). ^{29}Si NMR (99 MHz, C_6D_6) δ -21.34. Analysis calculated for $C_{30}H_{30}FeN_2Si$: C 71.71, H 6.02, N 5.57%. Found: C 71.71, H 5.86, N 5.43%.

General synthetic procedure for P1-P4. In the glove box, a 5 ml solution of 1.05 g **1** (3.6 mmol) and 0.49 g *p*-xylylenediamine (3.6 mmol) was made up in toluene (0.72 M) and stirred overnight before use to ensure complete dissolution. A Schlenk flask was charged with 1 ml of the stock solution (0.72 mmol) and heated to 60°C. The catalyst was added to another Schenk flask, dissolved in 0.5 ml toluene, and added *via* cannula to the monomer solution. Immediate and vigorous effervescence was accompanied by the appearance of an intense purple colour, and the reaction was stirred at 60°C for a further 2 hours to ensure complete conversion. Polymers were isolated by precipitation into pentane at -78°C, cannula filtration, and removal of solvent under vacuum. Although every effort was made to remove all traces of solvent from polymers **P1**-**P4**, substantial quantities of entrapped toluene were observed, and prevented meaningful elemental analysis from being obtained.

Synthesis of polymer P1. Polymer **P1** was synthesised according to the general procedure, using 21.6 mg **III** (0.035 mmol, 5 mol%). Isolated yield following precipitation: 0.105 g, 33%. ^{1}H NMR (500 MHz, C_6D_6) δ 7.88 (d, *J* = 6.6 Hz, 49H, *o-Ph*Si), 7.38 (s, 91H, H_c), 7.29 (q, *J* = 7.7, 7.0 Hz, 88H, *m,p-Ph*Si), 4.37 – 4.07 (m, 197H, H_d + Si*Cp*), 3.96 (s, 114H, *Cp*), 3.61 (t, *J* = 7.2 Hz, 4H, H_b), 1.49 (t, *J* = 7.8 Hz, 54H, H_e), 0.77 (s, 4H, H_a). ^{13}C NMR (126 MHz, C_6D_6) δ 142.83 (C_2), 138.12 (*i-Ph*Si), 135.07 (*o-Ph*Si), 129.75 (*m-Ph*Si), 128.35 (*p-Ph*Si), 127.52 (C_3), 74.37 (2,5-*Cp*Si), 71.39 (3,4-*Cp*Si), 68.92 (*Cp*), 68.64 (1-*Cp*Si), 45.95 (C_1, C_4). ^{29}Si NMR (99 MHz, C_6D_6) δ -21.46.

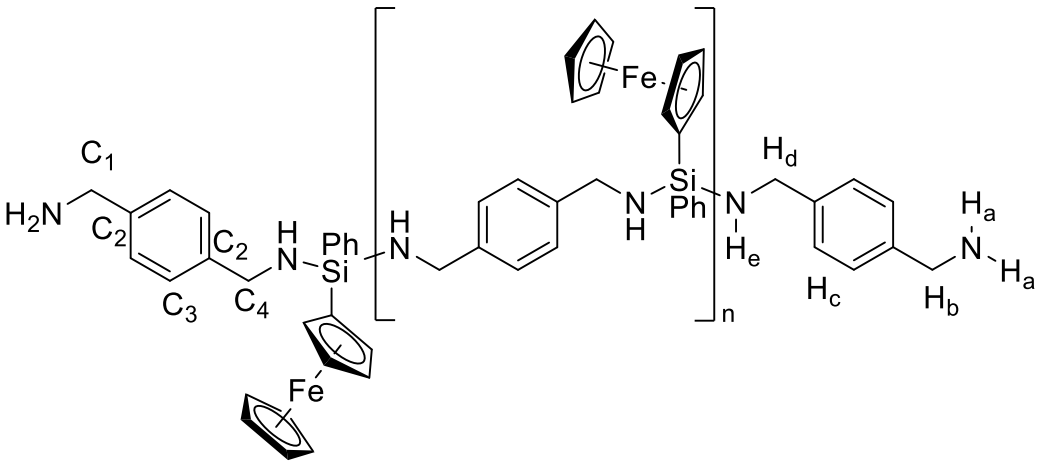

Synthesis of polymer P2. Polymer **P2** was synthesised according to the general procedure, using 14.3 mg **III** (0.024 mmol, 3.3 mol%). Isolated yield following precipitation: 0.172 g, 57%. ^{1}H NMR (500 MHz, C_6D_6) δ 7.88 (dq, *J* = 5.7, 2.1 Hz, 50H, *o-Ph*Si), 7.38 (s, 81H, H_c), 7.35 – 7.23 (m, 81H, *m,p-Ph*Si), 4.30 – 4.14 (m, 183H, H_d + Si*Cp*), 3.96 (s, 104H, *Cp*), 3.61 (t, *J* = 7.0 Hz, 4H, H_b), 1.49 (t, *J* = 7.9 Hz, 54H, H_e), 0.77 (s, 4H, H_a). ^{13}C NMR (126 MHz, C_6D_6) δ 142.83 (C_2), 138.12 (*i-Ph*Si), 135.08 (*o-Ph*Si), 129.75 (*m-Ph*Si), 128.35 (*p-Ph*Si), 127.52 (C_3), 74.37 (2,5-*Cp*Si), 71.39 (3,4-*Cp*Si), 68.92 (*Cp*), 68.64 (1-*Cp*Si), 45.95 (C_1, C_4). ^{29}Si NMR (99 MHz, C_6D_6) δ -21.46.

Synthesis of polymer P3. Polymer **P3** was synthesised according to the general procedure, using 4.3 mg **III** (0.007 mmol, 1 mol%). Isolated yield following precipitation: 0.200 g, 62%. ^{1}H NMR (500 MHz, C_6D_6) δ 7.87 – 7.80 (m, 5H, *o*-Si*Ph*), 7.80 – 7.75 (m, 2H, *o*-Si*Ph*), 7.33 (dd, *J* = 5.5, 1.8 Hz, 5H, H_c), 7.31 – 7.19 (m, 12H, *m,p-Ph*Si), 5.91 (d, *J* = 5.7 Hz, 0H, Si*H*), 5.63 (t, *J* = 2.3 Hz, 1H, Si*H*), 5.10 (s, 0H, Si*H*), 4.25 – 4.09 (m, 23H, Si*Cp* + H_d), 3.99 – 3.94 (m, 2H, H_d), 3.94 – 3.92 (m, 2H, *Cp*), 3.92 – 3.90 (m, 8H, *Cp*), 3.56 (q, *J* = 6.8 Hz, 4H, H_b), 1.53 – 1.39 (m, 5H, H_e), 1.08 (t, *J* = 8.2 Hz, 0H, H_e), 0.72 (s, 4H, H_a). ^{13}C NMR (126 MHz, C_6D_6) δ 142.83 (C_2), 142.29 (C_2), 138.12 (*i-Ph*Si), 135.06 (*o-Ph*Si), 130.09 (*m-Ph*Si), 129.74 (*m-Ph*Si), 128.35 (*p-Ph*Si), 127.51 (C_3), 127.49 (C_3), 127.40 (C_3), 74.58 (2,5-*Cp*Si), 74.35 (2,5-*Cp*Si), 71.87 (3,4-*Cp*Si), 71.73 (3,4-*Cp*Si), 71.37 (3,4-*Cp*Si), 68.90 (*Cp*), 68.63 (1-*Cp*Si), 46.58 (C_1), 45.93 (C_4). ^{29}Si NMR (99 MHz, C_6D_6) δ -21.45.

Synthesis of polymer P4. Polymer **P6** was synthesised according to the general procedure, using 14.3 mg **VI** (0.024 mmol, 3.3 mol%). Isolated yield following precipitation: 0.192 g, 63%.^{1}H NMR (500 MHz, C_6D_6) δ 7.92 – 7.83 (m, 64H, *o-Ph*Si), 7.38 (s, 104H, H_c), 7.34 – 7.24 (m, 99H, *m,p-Ph*Si), 4.30 – 4.12 (m, 223H, H_d + Si*Cp*), 3.96 (s, 128H, *Cp*), 3.61 (t, *J* = 7.1 Hz, 4H, H_b), 1.49 (t, *J* = 7.8 Hz, 70H, H_e), 0.77 (s, 3H, H_a). ^{13}C NMR (126 MHz, C_6D_6) δ 142.83 (C_2), 138.12 (*i-Ph*Si), 135.07 (*o-Ph*Si), 129.75 (*p-Ph*Si), 128.35 (*m-Ph*Si), 127.52 (C_3), 74.37

(2,5-*Cp*Si), 71.39 (3,4-*Cp*Si), 68.92 (*Cp*), 68.64 (1-*Cp*Si), 45.95 (C_1, C_4). ^{29}Si NMR (99 MHz, C_6D_6) δ -21.45.

Synthesis of polymer P5. A Schenk flask was charged with 0.105 g **1** (0.36 mmol), 0.049 g *p*-xylylenediamine (0.36 mmol), and 0.25 ml THF. The monomer solution was stirred for 1 hour until completely dissolved before a THF solution of **III** was added (7.1 mg, 0.012 mmol, 3.3 mol%, in 0.02 ml THF). Immediate and vigorous effervescence was accompanied by the appearance of an intense purple colour. The reaction was stirred for a further hour, before the viscous solution was diluted with a further 0.5 ml THF and precipitated into non-dried hexane. The polymer was isolated as a pale orange solid following filtration and removal of solvent under vacuum. Yield 60.5 mg, 39.6%. ^{1}H NMR (500 MHz, C_6D_6) δ 7.92 – 7.84 (m, 55H, *o*-*Ph*Si), 7.38 (s, 90H, H_c), 7.33 – 7.24 (m, 86H, *m,p*-*Ph*Si), 4.29 – 4.12 (m, 223H, H_d + Si*Cp*), 3.96 (s, 108H, *Cp*), 3.61 (t, *J* = 7.1 Hz, 4H, H_b), 1.49 (t, *J* = 7.8 Hz, 63H, H_e), 0.77 (s, 4H, H_a). ^{13}C NMR (126 MHz, C_6D_6) δ 142.83 (C_2), 138.12 (*i*-*Ph*Si), 135.07 (*o*-*Ph*Si), 129.75 (*p*-*Ph*Si), 128.35 (*m*-*Ph*Si) 127.52 (C_3), 74.37 (2,5-*Cp*Si), 71.39 (3,4-*Cp*Si), 68.93 (*Cp*), 68.64 (1-*Cp*Si), 45.95 (C_1, C_4). ^{29}Si NMR (99 MHz, C_6D_6) δ -21.45.

Synthesis of polymer P6. A Schenk flask was charged with 0.126 g **1** (0.43 mmol), 0.059 g *p*-xylylenediamine (0.43 mmol), and 0.6 ml toluene. The monomer solution was stirred for 1 hour until completely dissolved before a toluene solution of **III** was added (8.7 mg, 0.014 mmol, 3.3 mol%, in 0.33 ml toluene). Immediate and vigorous effervescence was accompanied by the appearance of an intense purple colour. The reaction was stirred for two hours at room temperature before precipitating twice into non-dried hexane. The polymer was isolated as a pale orange solid following filtration and removal of solvent under vacuum. Yield 90.6 mg, 49.6%. ^{1}H NMR (500 MHz, C_6D_6) δ 7.88 (dt, *J* = 5.9, 2.3 Hz, 92H, *o*-*Ph*Si), 7.38 (s, 180H, H_c), 7.33 – 7.23 (m, 171H, *m* + *p*-*Ph*Si), 4.29 – 4.14 (m, 369H, H_d + Si*Cp*), 3.96 (s, 206H, *Cp*), 3.61 (t, *J* = 6.9 Hz, 4H, H_b), 1.49 (t, *J* = 7.8 Hz, 92H, H_e), 0.77 (s, 4H, H_a). ^{13}C NMR (126 MHz, C_6D_6) δ 142.83 (C_2), 138.12 (*i*-Si*Ph*), 135.07 (*o*-Si*Ph*), 129.75 (*p*-Si*Ph*), 128.14 (*m*-Si*Ph*), 127.52 (C_3), 74.37 (2,5-Si*Cp*), 71.39 (3,4-Si*Cp*), 68.93 (*Cp*), 68.64 (1-Si*Cp*), 45.95 (C_4). ^{29}Si NMR (99 MHz, C_6D_6) δ -21.45.

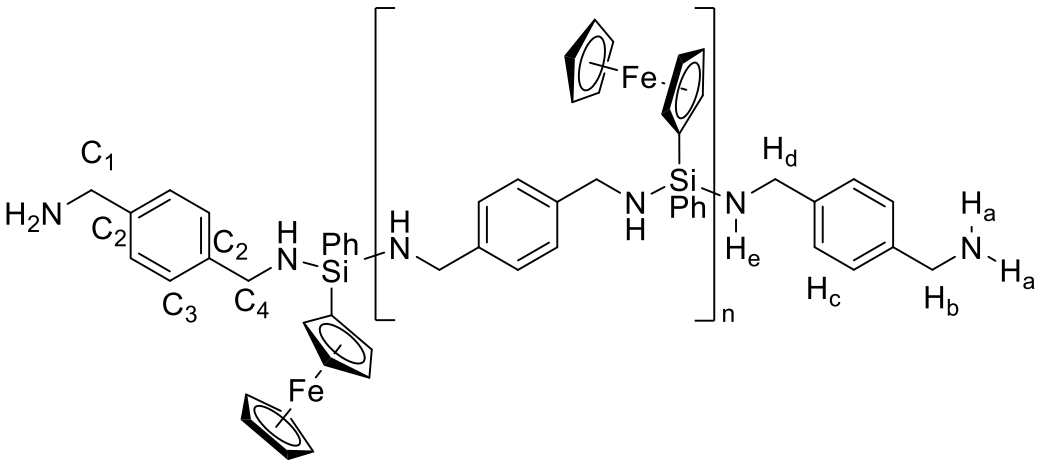

Synthesis of polymers P7a and P7b. A Schenk flask was charged with 0.126 g **1** (0.43 mmol), 0.059 g *p*-xylylenediamine (0.43 mmol), and 0.6 ml toluene. The monomer solution was stirred for 1 hour until completely dissolved before a toluene solution of **III** was added (8.7 mg, 0.014 mmol, 3.3 mol%, in 0.33 ml toluene). Immediate and vigorous effervescence was accompanied by the appearance of an intense purple colour. After stirring for two hours at room temperature, half of the reaction mixture was removed and precipitated twice into non-dried hexane, yielding **P7a** 13.9 mg (7.6%). ^{1}H NMR (500 MHz, C_6D_6) δ 7.91 – 7.83 (m, 75H, *o*-*Ph*Si), 7.38 (d, *J* = 2.0 Hz, 126H, H_c), 7.29 (d, *J* = 7.3 Hz, 104H, *m* + *p*-*Ph*Si), 4.28 – 4.13 (m, 293H, H_d + Si*Cp*), 3.96 (d, *J* = 2.2 Hz, 139H, *Cp*), 3.61 (t, *J* = 7.1 Hz, 4H, H_b), 1.50 (t, *J* = 7.7 Hz, 78H, H_e), 0.77 (s, 4H, H_a). ^{13}C NMR (126 MHz, C_6D_6) δ 142.84 (C_2), 138.12 (*i*-Si*Ph*), 135.08 (*o*-Si*Ph*), 129.75 (*p*-Si*Ph*), 128.15 (*m*-Si*Ph*), 127.52 (C_3), 74.37 (2,5-Si*Cp*), 71.39 (3,4-Si*Cp*), 68.93 (*Cp*), 68.64 (1-Si*Cp*), 45.95 (C_4). ^{29}Si NMR (99 MHz, C_6D_6) δ -21.45.

A further 4.4 mg **III** (0.007 mmol) in 0.150 ml toluene was added without further visual change. The reaction was stirred for a further two hours before precipitating twice into non-dried hexane to yield **P7b** 30.3 mg (16.6%). NMR spectra were very similar to that of **P7b**. ^{1}H NMR (500 MHz, C_6D_6) δ 7.93 – 7.82 (m, 60H), 7.38 (s, 89H), 7.34 – 7.24 (m, 89H), 4.30 – 4.11 (m, 226H), 3.96 (s, 126H), 3.61 (t, *J* = 6.8 Hz, 4H), 1.49 (t, *J* = 7.8 Hz, 63H), 0.77 (s, 4H). ^{13}C NMR (126 MHz, C_6D_6) δ 142.83, 138.12, 135.08, 129.75, 128.14, 127.52, 74.37, 71.39, 68.92, 68.64, 45.95. ^{29}Si NMR (99 MHz, C_6D_6) δ -21.46.

Synthesis of Fe(CpSiPhH$_2$)$_2$ 3. In the glove box, a Schlenk flask was charged with 3.26 g ferrocene (18 mmol) and 6.45 ml *N,N,N'N'*-tetramethylethylenediamine (TMEDA) (43 mmol). Another Schlenk flask was charged with 17.0 ml 2.5 M nBuLi in hexanes (43 mmol). The ferrocene and TMEDA were dissolved/suspended in ~80 ml hexane, and on the Schlenk line, the nBuLi solution was added dropwise with stirring. The reaction mixture was stirred at room temperature for 16 hours and the resultant pale orange suspension allowed to settle before

cannula filtration. The pale orange solid (dilithioferrocene) was washed with two portions of hexane, then re-suspended in ~50 ml fresh hexane. The suspension was cooled to 0 °C, and 4.7 ml $SiPhH_2Cl$ (35 mmol) was added dropwise. The reaction was allowed to reach room temperature, and stirred for a further 16 hours. The product was extracted from the LiCl by-product with hexane, cannula filtered, and solvent removed under reduced pressure to obtain a sticky orange residue. Prolonged sublimation onto a dry-ice cold finger and the walls of a Schlenk flask at 140 °C yielded the pure product as orange crystals suitable for single-crystal X-ray diffraction analysis, 1.98 g, 28.4% yield. ^{1}H NMR (300 MHz, C_6D_6) δ 7.65 – 7.56 (m, 4H, *o*-C_6H_5), 7.20 – 7.09 (m, 6H, *m,p*-C_6H_5), 5.10 (s, 4H, SiH_2), 4.20 (t, *J* = 1.7 Hz, 4H, 2,5-Cp*H*), 4.13 (t, *J* = 1.9 Hz, 4H, 3,4-Cp*H*). ^{13}C NMR (126 MHz, C_6D_6) δ 135.56 (*o*-Ph), 133.24 (*i*-Ph), 129.97 (*m*-Ph), 128.39 (*p*-Ph), 75.83 (3,4-Cp), 72.92 (2,5-Cp), 61.91 (1-Cp). ^{29}Si NMR (99 MHz, C_6D_6) δ -35.83. Analysis calculated for $C_{22}H_{22}Si_2Fe$: C 66.32 H 5.57 N 0.00%. Found: C 66.27, H 5.48, N 0.00%.

Reaction of benzyl amine with 1,1'-bis(phenylsilyl)ferrocene 3 to yield 4. To a J. Youngs NMR tube was added 10 mg **3** ($2.5x10^{-5}$ mol), 5.48 µl benzyl amine ($5x10^{-5}$ mol), and 0.5 ml C_6D_6. 1.5 mg **III** ($2.5x10^{-6}$ mol) was dissolved in 0.1 ml C_6D_6 and added to the NMR tube. The reaction mixture was heated to 60°C for 16 hours, after which no further reaction was observed. Multinuclear NMR of the crude reaction mixture revealed a mixture of reaction products, precluding detailed characterisation. Solvent was removed under vacuum, and the crude product was re-dissolved in a hexane/toluene mixture. Cooling to -30°C resulted in the isolation of orange crystalline blocks, identified by single crystal X-ray diffraction analysis as compound **4**. Yield 0.5 mg, 2.4%. The reaction was also carried out following the same procedure, but with a 1:2 Si:N ratio; **3** (10 mg, $2.5x10^{-5}$ mol) and benzyl amine ($1.0x10^{-4}$ mol). In this case, a higher yield of crystals were obtained, enabling full characterisation by NMR spectroscopy and elemental microanalysis. Yield 4.0 mg, 19.5% ^{1}H NMR (500 MHz, C_6D_6) δ 7.83 – 7.75 (m, 4H, o-SiPh), 7.30 – 7.22 (m, 14H, *m*+*p*-Si*Ph*, *o*-NHCH2*Ph*), 7.19 (dd, *J* = 8.4, 6.8 Hz, 8H, *m*-NHCH2*Ph*), 7.13 – 7.07 (m, 4H, *p*-NHCH2*Ph*), 4.13 (t, J = 1.7 Hz, 4H, *2,5-Cp*), 4.12 (t, J = 1.6 Hz, 4H, *3,*4-*Cp*), 4.06 (d, J=1.7 Hz, 4H, NHC*H2*), 4.04 (s, br, 4H, NHC*H2*), 1.41 (t, *J* = 8.0 Hz, 4H, N*H*). ^{13}C NMR (126 MHz, C_6D_6) δ 144.46 (*i*-NHCH2*Ph*), 137.84 (*i*-Si*Ph*), 135.03 (*o*-Si*Ph*), 129.81 (*m*-Si*Ph*), 128.62 (*m*-NHCH2*Ph*), 127.39 (*m*-NHCH2*Ph*), 126.76 (*p*-NHCH2*Ph*), 74.65 (*3,4-Cp*), 72.22 (*2,5-Cp*), 68.86 (*1-Cp*), 46.02 (*C*H2). ^{29}Si NMR (99 MHz, C_6D_6) δ -21.32. Analysis calculated for $C_{50}H_{50}FeN_4Si_2$: C 73.33, H 6.15, N 6.84%. Found: C 73.28, H 6.35, N 6.66%.

Synthesis of P8. To a Schlenk flask was added 120 mg **3** (0.3 mmol), 41 mg *p*-xylylenediamine (0.3 mmol), and 2 ml toluene. 9 mg **III** (0.015 mmol) was dissolved in 1 ml toluene and added to the monomer solution resulting in immediate effervescence and a colour change to purple. After heating to 60°C for 16 hours to ensure complete conversion, the reaction was quenched by addition of 1 ml non-dried hexane. After prolonged drying under vacuum, the product was recovered as a pale orange powder, 105 mg, 60%. ^{1}H NMR (500 MHz, C_6D_6) δ 8.12 – 7.63 (m, 390H *o*-Si*Ph*), 7.52 – 7.19 (m, 1015H, *m,p*-Si*Ph* + C_6H_4), 5.88 – 5.75 (m, 63H, Si*H*), 5.73 (s, 22H, Si*H*), 5.64 (d, *J* = 6.1 Hz, 19H, Si*H*), 5.56 (d, *J* = 9.7 Hz, 8H, Si*H*), 4.61 – 3.80 (m, 1230H, *Cp* + CH_2), 3.58 (br, s, 1H, CH_2NH_2), 3.51 (t, 2H, CH_2NH_2), 1.75 – 1.03 (m, 131H, N*H*). ^{13}C NMR (126 MHz, C_6D_6) δ 139.84 (*i*-Si*Ph*), 135.19 (*o*-Si*Ph*), 135.17 (*o*-Si*Ph*), 135.13 (*o*-Si*Ph*), 135.10 (*o*-Si*Ph*), 135.08 (*o*-Si*Ph*), 130.08 (Si*Ph*), 129.96 (*p*-Si*Ph*), 129.10 (*Ar*), 128.92 (*m*-Si*Ph*), 127.54 (C_6H_4), 127.07 (C_6H_4), 76.73 (2,4-*Cp*), 76.60 (2,4-*Cp*), 76.52 (2,4-*Cp*), 75.36 (*Cp*), 74.50 (*Cp*), 74.35 (*Cp*), 73.67 (*Cp*), 73.57 (*Cp*), 73.45 (*Cp*), 73.23 (*Cp*), 72.89 (*Cp*), 63.42 (1-*Cp*), 63.29 (1-*Cp*), 51.27 (*C*H2). ^{29}Si NMR (99 MHz, C_6D_6) δ -14.20.

General synthetic procedure for polymers P9-P10. In the glovebox, a 3.33 ml of **3** (0.96 g, 2.4 mmol) and *p*-xylylenediamine (0.33 g, 2.4 mmol) was made up in toluene (0.72 M) and stirred overnight to aid dissolution. A Schlenk flask was charged with 0.6 ml of the stock solution (0.43 mmol) and heated to 60°C. The catalyst was added to another Schenk flask, dissolved in 0.5 ml toluene, and added *via* cannula to the monomer solution. Immediate and vigorous effervescence was accompanied by the appearance of an intense purple colour, and the reaction was stirred at 60°C for a further 2 hours to ensure complete conversion. Polymers were isolated by precipitation into pentane at -78°C, cannula filtration, and removal of solvent under vacuum.

Synthesis of polymer P9. Polymer **P9** was synthesised according to the general procedure, using 13.1 mg **III** (0.022 mmol, 5 mol%). Isolated yield following precipitation: 0.110 g, 48%. ^{1}H NMR (500 MHz, C_6D_6) δ 7.97 – 7.63 (m, 44H, *o*-Si*Ph*), 7.47 – 7.19 (m, 143H, *m,p*-Si*Ph* + C_6H_4), 5.79 (s, br 6H, Si*H*), 5.74 (s, 0H, Si*H*), 5.72 (s, 0H, Si*H*), 5.62 (d, *J* = 11.3 Hz, 7H, Si*H*), 4.60 – 4.38 (m, 10H, *Cp*), 4.38-4.31 (m, 9H, CH_2), 4.31 – 3.89 (m, 137H, *Cp* + CH_2), 3.85 (s, 4H, CH_2), 3.60 (s, 4H, CH_2NH_2), 3.51 (s, 1H, CH_2NH_2), 1.45 (d, *J* = 32.6 Hz, 9H, N*H*), 1.10 (s, 3H, N*H*), 0.76 (s, 3H, NH_2). ^{13}C NMR (126 MHz, C_6D_6) δ 135.17 (*o*-Si*Ph*), 135.08 (*o*-Si*Ph*), 135.06 (*o*-Si*Ph*), 76.71 (*Cp)*, 74.35 (*Cp)*, 73.66 (*Cp)*, 72.88 (*Cp)*, 63.28 (1-*Cp*), 51.22 (CH_2), 47.00 (CH_2), 45.89 (CH_2). ^{29}Si NMR (99 MHz, C_6D_6, determined from ^{1}H-^{29}Si HMQC) δ -14.15

Synthesis of polymer P10. Polymer **P10** was synthesised according to the general procedure, using 8.7 mg **III** (0.014 mmol, 3.3 mol%). Isolated yield following precipitation: 0.120 g, 52%. ^{1}H NMR (500 MHz, C_6D_6) δ 7.92 – 7.68 (m, 28H, *o*-Si*Ph*), 7.43 – 7.19 (m, 58H, *m,p*-Si*Ph* + C_6H_4), 5.79 (s, 3H, Si*H*), 5.74 (s, 0H, Si*H*), 5.73 (s, 0H, Si*H*), 5.66 – 5.55 (m, 8H, Si*H*), 4.44 (s, 1H), 4.41 (s, 4H), 4.33 (m, CH_2), 4.31 – 3.89 (m, 79H, *Cp* + CH_2), 3.86 (d, *J* = 7.8 Hz, 2H, CH_2), 3.59 (s, 4H, CH_2NH_2), 3.51 (s, 1H, CH_2NH_2), 1.91 – 1.26 (m, 87H, N*H*), 1.06 (d, *J* = 47.1 Hz, 8H, N*H*), 0.76 (s, 3H, N*H*), 0.44 (s, 22H, N*H*). ^{13}C NMR (126 MHz, C_6D_6) δ 142.29 (1-C_6H_4), 142.20 (1-C_6H_4), 135.16 (*o*-Si*Ph*), 135.07 (*o*-Si*Ph*), 135.05 (*o*-Si*Ph*), 130.14 (*m*-Si*Ph*), 129.02 (Si*Ph*), 127.47 (2,5-C_6H_4), 127.05 (2,5-C_6H_4), 76.70 (*Cp)*, 75.84 (*Cp)*, 75.35 (*Cp)*, 75.31 (*Cp)*, 75.17 (*Cp)*, 75.11 (*Cp)*, 74.80 (*Cp)*, 74.35 (*Cp)*, 74.22 (*Cp)*, 74.10 (*Cp)*, 73.66 (*Cp)*, 73.46 (*Cp)*, 72.88 (*Cp)*, 72.54 (*Cp)*, 72.51 (*Cp)*, 72.42 (*Cp)*, 47.01 (CH_2). ^{29}Si NMR (99 MHz, C_6D_6, determined from ^{1}H-^{29}Si HMQC) δ -14.13, -16.24.

Attempted polymerisation of 3 and *p*-xylylenediamine using 1 mol% III. The experiment was carried out according to the general procedure, using 2.6 mg **III** (0.0043 mmol, 1 mol%). The ^{1}H NMR spectrum of the product showed predominantly starting material, and no polymeric products by DOSY (See supporting information: Figure S106, Figure S107).

Reaction of 1,1'-bis(amino)ferrocene with Ph_2SiH_2 to yield 5. To a J. Youngs NMR tube was added 10 mg $Fe(CpNH_2)_2$ **VII** (4.63×10^{-5} mol), 17.2 µl diphenylsilane (9.26×10^{-5} mol), and 0.5 ml d_8-THF. 1.4 mg **III** (2.31×10^{-6} mol) was dissolved in 0.1 ml d_8-THF in a vial, and transferred to the NMR tube. On heating to 60°C for 16 hours, complete consumption of **VII** was obtained. Compound **5** was isolated in the form of large orange blocks suitable for single crystal X-ray diffraction by subjecting a THF solution to hexane diffusion at room temperature. Isolated yield 8.6 mg, 47.5%. ^{1}H NMR (500 MHz, C_6D_6) δ 7.80 – 7.73 (m, 4H, *o-Ph*), 7.25 – 7.16 (m, 6H, *m,p-Ph*), 3.82 (t, *J* = 1.9 Hz, 4H, 2,4-*Cp*), 3.80 (t, *J* = 1.8 Hz, 4H, 3,5-*Cp*), 2.09 (s, 2H, N*H*). ^{13}C NMR (126 MHz, C_6D_6) δ 135.83 (*i-Ph*), 135.57 (*o-Ph*), 130.47 (*m-Ph*), 128.35 (*p-Ph*), 97.95 (1-*Cp*), 66.16 (3,5-*Cp*), 65.93 (2,4-*Cp*). ^{29}Si NMR (99 MHz, C_6D_6) δ -16.08. Analysis calculated for $C_{22}H_{20}FeN_2Si$: C 66.67, H. 5.09, N 7.07%. Found: C 66.48, H 5.16, N 6.91%. Melting point 200°C (DSC).

This reaction was also carried out using the same method, but with 4.6 mg **VII** (2.10×10^{-5} mol), 2.89 µl diphenylsilane (2.10×10^{-5} mol), and 0.7 mg **III** (1.16×10^{-6} mol), yielding the same product in 95% spectroscopic yield. The product was not isolated in this case.

Synthesis of RuCp(Cp($SiPhH_2$)) 6. A Schlenk flask was charged with 0.98 g ruthenocene (4.23 mmol) and 59 mg KOtBu (0.53 mmol), dissolved in THF, and cooled to -78°C. Another

Schlenk was charged with 5 ml tBuLi (1.7 M solution in pentane), which was added dropwise to the ruthenocene solution *via* cannula. The reaction mixture was stirred at -78°C for a further 30 minutes before 1.3 ml $PhSiH_2Cl$ (9.75 mmol) was slowly added. After removing from the cold bath, the reaction was stirred for 90 minutes. The solvent was removed under reduced pressure, and the product was extracted twice with hexane. The crude product was obtained as a yellow residue following removal of solvent under vacuum. The pure product was collected as an off-white crystalline solid by sublimation at 65°C. A colourless plate obtained from the sublimation was selected for single crystal X-ray diffraction analysis. ^{1}H NMR (300 MHz, C_6D_6) δ 7.69 – 7.59 (m, 3H, *m,p*-C_6H_5), 7.24 – 7.17 (m, 2H, *o*-C_6H_5), 5.11 (s, *J* = 1.5 Hz, 2H, SiH_2), 4.60 (t, *J* = 1.5 Hz, 2H, 2,5-SiCp*H*), 4.55 (t, *J* = 1.7 Hz, 2H, 3,4-SiCp*H*), 4.40 (s, 5H, Cp*H*). ^{13}C{^{1}H} NMR (126 MHz, C_6D_6) δ 135.11 (*o*-C_6H_5), 133.45 (*i*-C_6H_5) 129.49 (*m*-C_6H_5), 127.92 (*p*-C_6H_5), 76.26 (3,4-SiCp), 73.34 (2,5-SiCp), 70.93 (Cp). ^{29}Si NMR (99 MHz, C_6D_6) δ -36.82. Analysis calculated for $C_{16}H_{16}RuSi$: C 56.95, H 4.78, N 0.00%. Found: C 57.07, H 4.90, N 0.00%.

Reaction of 1,1'-bis(amino)ferrocene with RuCp(Cp(SiPhH_2)) 6 to yield 7. To a J. Youngs NMR tube was added 4.9 mg **VII** ($2.2x10^{-5}$ mol), 7.0 mg **6** ($2.1x10^{-5}$ mol), and 0.5 ml d_8-THF. 0.6 mg **III** ($1x10^{-6}$ mol) was dissolved in 0.1 ml d_8-THF in a vial, and transferred to the NMR tube. After heating to 60°C for 16 hours, complete conversion was obtained, with 80% spectroscopic yield of the ferrocenophane product **7**. Addition of a hexane layer to the NMR tube yielded crystals suitable for single crystal X-ray diffraction analysis on standing at room temperature for several days, isolated: 3 mg, 23% yield. ^{1}H NMR (500 MHz, d_8-THF) δ 7.96 – 7.88 (m, 2H, *o-Ph*), 7.46 – 7.39 (m, 3H, *m,p-Ph*), 4.64 (t, *J* = 1.6 Hz, 2H, 2,5-Ru*Cp*Si), 4.50 (t, *J* = 1.6 Hz, 2H, 3,4-Ru*Cp*Si), 4.49 (s, 5H, Ru*Cp*), 3.99 (dt, *J* = 2.5, 1.4 Hz, 2H, 2-Fe*Cp*), 3.72 (tt, *J* = 2.2, 1.1 Hz, 2H, 3-Fe*Cp*), 3.65 (dt, *J* = 2.5, 1.4 Hz, 2H, 5-Fe*Cp*), 3.35 (dt, *J* = 2.6, 1.4 Hz, 2H, 4-Fe*Cp*), 2.88 (s, 2H, N*H*). ^{13}C{^{1}H} point NMR (126 MHz, d_8-THF) δ 138.70 (*i-Ph*), 136.62 (*o-Ph*), 130.44 (*m-Ph*), 128.23 (*p-Ph*), 99.86 (1-Fe*Cp*), 75.95 (3,4-Ru*Cp*Si), 73.32 (2,5-Ru*Cp*Si), 71.71 (Ru*Cp*), 70.99 (1-Ru*Cp*Si) 69.13 (2-Fe*Cp*), 65.99 (, 5-Fe*Cp*), 64.84 (3-Fe*Cp*), 62.72 (4-Fe*Cp*). ^{29}Si NMR (99 MHz, d_8-THF) δ -7.41. Analysis calculated for $C_{26}H_{24}FeN_2RuSi$: C 56.84, H 4.40, N 5.10%. Found: C 56.61, H 4.27, N 5.13%. Melting point (DSC): 261°C.

Reaction of *N,N'*-dimethyl-*p*-xylylenediamine with two equivalents of diphenylsilane in the presence of III to yield 8. To a J. Youngs NMR tube was added 10 µl *N,N*'-dimethyl-*p*-xylyenediamine ($6.21x10^{-5}$ mol), 24.6 µl Ph_2SiH_2 ($1.24x10^{-4}$ mol), and 0.5 ml C_6D_6. 1.9 mg **III** ($3.15x10^{-6}$ mol) was dissolved in 0.1 ml C_6D_6 and added to the NMR tube. After heating to 60°C overnight, 90% of Ph_2SiH_2 was obtained, and after a further 24 hours at 80°C, complete

conversion resulted in near quantitative spectroscopic yield of **8**. Colourless blocks suitable for single crystal x-ray diffraction could be obtained by slow cooling a hot toluene solution to room temperature, or room temperature toluene solution to -30°C. Yield 13.4 mg, 40%. ^{1}H NMR (500 MHz, C_6D_6) δ 7.73 – 7.66 (m, 8H, *o*-Si*Ph*), 7.25 (s, 4H, $CH_2C_6H_4CH_2$), 7.23 – 7.18 (m, 12H, *m,p*-Si*Ph*), 5.69 (s, 2H, Si*H*), 4.00 (s, 4H, CH_2), 2.45 (s, 6H, NCH_3). ^{13}C NMR (126 MHz, C_6D_6) δ 139.34 (1-$CH_2C_6H_4CH_2$), 135.60 (*i*-S*Ph*), 135.48 (*o*-Si*Ph*), 129.91 (*m*-Si*Ph*), 128.42 (*p*-Si*Ph*), 128.31 (2,3-$CH_2C_6H_4CH_2$), 55.57 (NCH_2), 35.34 (NCH_3). ^{29}Si NMR (99 MHz, C_6D_6) δ -10.99. Analysis calculated for $C_{34}H_{36}N_2Si_2$: C 77.22, H 6.86, N 5.30%. Found: C 77.29, H 6.94, N 5.23%.

Synthesis of polymer P11. A Schlenk flask was charged with 48.3 µl *N,N*'-dimethyl-*p*-xylylenediamine (0.30 mmol), 120 mg **3** (0.30 mmol), and 4 ml toluene. 9 mg **III** (0.015 mmol) was dissolved in 1 ml toluene and added to the monomer solution. The reaction was heated to 60°C for 16 hours to ensure complete conversion. The reaction mixture was cooled to -78°C and precipitated by addition of a large excess of pentane. Following filtration and solvent removal under vacuum, the product was obtained as a pale orange solid, 0.084 g, 50% yield. ^{1}H NMR (500 MHz, C_6D_6) δ 7.80 (t, *J* = 7.4 Hz, 40H, *o-Ph*SiH), 7.68 – 7.52 (m, 5H, *o-Ph*SiH_2), 7.28 (dd, *J* = 9.7, 5.7 Hz, 94H, *m,p-Ph*Si, H_g), 5.68 (s, 2H, H_d), 5.64 (d, *J* = 59.3 Hz, 17H, H_h), 5.10 (d, *J* = 5.9 Hz, 2H, H_a), 5.04 (d, *J* = 6.0 Hz, 2H, H_a), 4.38 (s, 8H, *Cp*), 4.34 (s, 3H *Cp*), 4.31 – 4.08 (m, 70H, *Cp*), 4.01 (dd, *J* = 19.7, 13.0 Hz, 53H, H_f), 2.44 (s, 41H, H_e), 2.42 (s, 43H, H_e). ^{13}C NMR (126 MHz, C_6D_6) δ 139.54 (C_6), 136.99 (*i-Ph*Si), 136.95 (*i-Ph*Si), 135.59 (*p-Ph*Si), 135.17 (*o-Ph*Si), 135.12 (*o-Ph*Si), 135.10 (*o-Ph*Si), 130.11 (*m-Ph*Si), 130.06 (*m-Ph*Si), 128.35 (C_7), 75.83 (*Cp*), 75.74 (*Cp*), 75.67 (*Cp*), 75.62 (*Cp*), 75.31 (*Cp*), 75.26 (*Cp*), 75.23 (*Cp*), 72.99 (*Cp*), 72.86 (*Cp*), 72.75 (*Cp*), 72.69 (*Cp*), 66.22 (1-*Cp*), 55.20 (C_5), 35.24 (C_4), 35.22 (C_4). ^{29}Si NMR (99 MHz, C_6D_6) δ -10.23, -10.32.

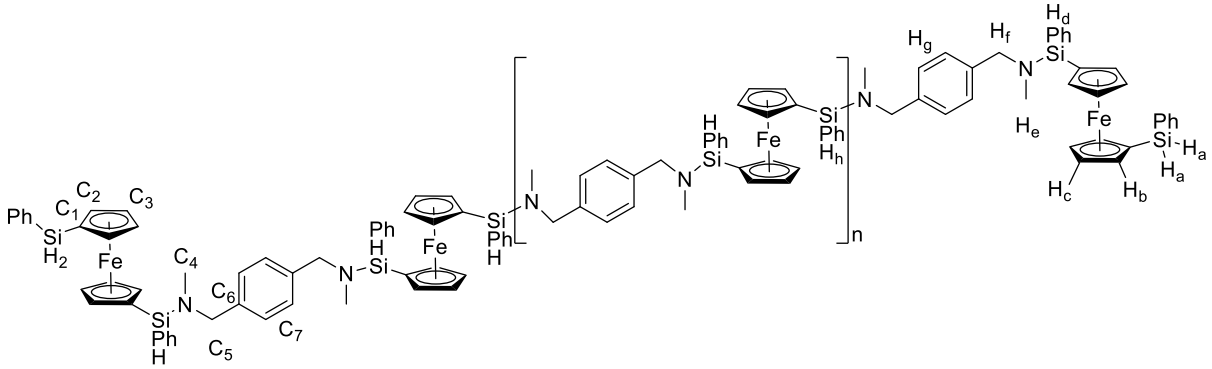

Synthesis of polymer P12. A Schlenk flask was charged with 0.6 ml of a 0.72 M solution (0.43 mmol) of *N,N*'-dimethyl-*p*-xylylenediamine and compound **3** in toluene. 12.9 mg **III** (0.022 mmol, 5 mol%) was dissolved in 0.33 ml toluene and added to the monomer solution,

resulting in immediate effervescence. After stirring at room temperature for 16 hours, the product was precipitated twice into non-dried hexane and obtained as a slightly sticky orange residue. 31.5 mg, 13% yield. ^{1}H NMR (500 MHz, C_6D_6) δ 7.85 – 7.73 (m, 126H, *o-Ph*SiH), 7.35 – 7.22 (m, 317H, *m,p-Ph*Si, H_e), 5.70 (d, *J* = 2.2 Hz, 29H, H_h), 5.58 (d, *J* = 2.1 Hz, 29H, H_h), 4.38 (s, 1H, 30), 4.23 (s, 60H, *Cp*), 4.22 – 4.18 (m, 62H, *Cp*), 4.17 (s, 33H, *Cp*), 4.15 (s, 31H, *Cp*), 4.07 – 3.91 (m, 168H, H_f), 3.54 (m, 4H, H_d) 2.43 (dd, *J* = 10.4, 2.4 Hz, 192H, H_g), 2.22 (d, J = 6.2 Hz, 6H, H_b) 0.62 (s, br, 2H, H_a). ^{13}C NMR (126 MHz, C_6D_6) δ 139.54 (C_3), 136.99 (*i-Ph*Si), 136.95 (*i-Ph*Si), 135.17 (*o-Ph*Si), 135.10 (*o-Ph*Si), 130.11 (*m-Ph*Si), 130.07 (*m-Ph*Si), 128.36 (*p*-Si*Ph*), 128.33 (C_4), 75.67 (*Cp*), 75.62 (*Cp*), 75.26 (*Cp*), 75.23 (*Cp*), 72.87 (*Cp*), 72.85 (*Cp*), 72.76 (*Cp*), 66.22 (1-*Cp*), 55.19 (C_2), 35.24 (C_1), 35.22 (C_1). ^{29}Si NMR (99 MHz, C_6D_6) δ -10.22, -10.32.

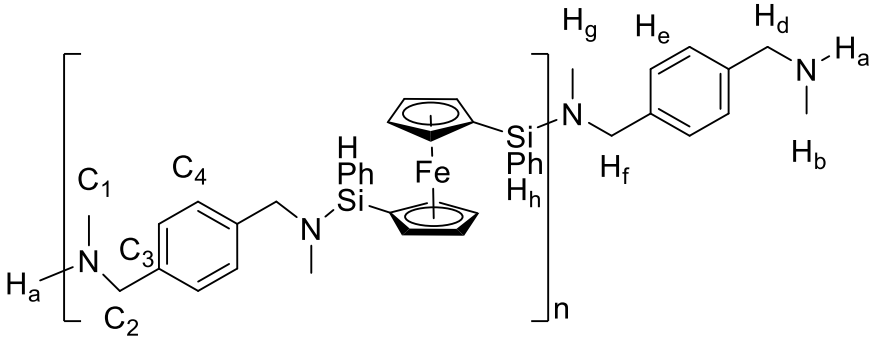

Synthesis of 1,1'-bis(dimethylsilyl)ferrocene IX. 1,1'-bis(dimethylsilyl)ferrocene was synthesised according to a modified literature procedure.[107, 108] A Schlenk flask was charged with 1.0 g ferrocene (5.5 mmol), 0.8 ml *N,N,N',N'*-tetramethylethylenediamine (5.3 mmol), and hexane. The mixture was stirred at room temperature, and 4.3 ml *n*BuLi (2.5 M in hexanes, 11 mmol) was added. After stirring at room temperature overnight, the yellow suspension was filtered and the 1,1'-dilithioferrocene product washed with toluene. The yellow solid was re-suspended in fresh toluene, cooled to 0°C, and 1.21 ml dimethylchlorosilane was added dropwise. The reaction mixture was allowed to warm to room temperature and stirred for 16 hours. After filtering and washing the LiCl byproduct with toluene, the solvent was removed under vacuum to yield the crude product as an orange oil. The product was purified by flash column chromatography using a hexane eluent and silica stationary phase. The products eluted as a broad orange band and collected as nine fractions, of which the first five contained the desired product in >98% purity. Isolated yield: 0.617 g, 37.1%. ^{1}H NMR (500 MHz, C_6D_6) δ 4.68 (hept, *J* = 3.7 Hz, 2H, Si*H*), 4.24 – 4.18 (m, 4H, 2,5-*Cp*), 4.05 (t, *J* = 1.7 Hz, 4H, 3,4-*Cp*), 0.27 (d, *J* = 3.7 Hz, 12H, CH_3). ^{13}C NMR (126 MHz, C_6D6) δ 74.03 (3,4-*Cp*), 71.93 (2,5-*Cp*), 68.32 (1-*Cp*), -2.87 (CH_3). ^{29}Si NMR (99 MHz, C_6D6) δ -18.68.

Synthesis of polymer P13. A Schlenk flask was charged with 25.2 mg *p*-xylylenediamine (0.185 mmol), 50µl **IX** (0.185 mmol), and 0.2 ml THF. 3.7 mg **III** (0.006 mmol) was dissolved in 0.05 ml THF and added to the monomer solution. The reaction mixture immediately became a deep purple colour and bubbled enthusiastically. After stirring at room temperature for 16 hours, the solution was diluted with 1.5 ml THF and precipitated into non-dried hexane at -78°C. Following filtration and removal of solvent under vacuum, the product was obtained as a sticky orange residue. Isolated yield 56.5 mg, 70.3 %. ^{1}H NMR (500 MHz, C_6D_6) δ 7.30 (s, br, 35H, Ar*H*), 4.26 (q, *J* = 1.9 Hz, 35H 2,5-*Cp*), 4.16 – 4.06 (m, 35H, 3,4-*Cp*), 3.94 (d, *J* = 8.0 Hz, 44H, H_c), 3.62 (t, *J* = 7.2 Hz, 4H, H_b), 0.81 (t, *J* = 8.0 Hz, 25H, H_d + H_a), 0.36 (s, br, 127H, C*H3*). ^{13}C NMR (126 MHz, C_6D_6) δ 142.92 (*1*-C_6H_4), 127.38 (2,6-C_6H_4), 73.59 (3,4-*Cp*), 71.79 (2,5-*Cp*), 46.61 (C_1), 46.33 (C_2), -0.15 (CH_3). ^{29}Si NMR (99 MHz, C_6D_6) δ -1.71.

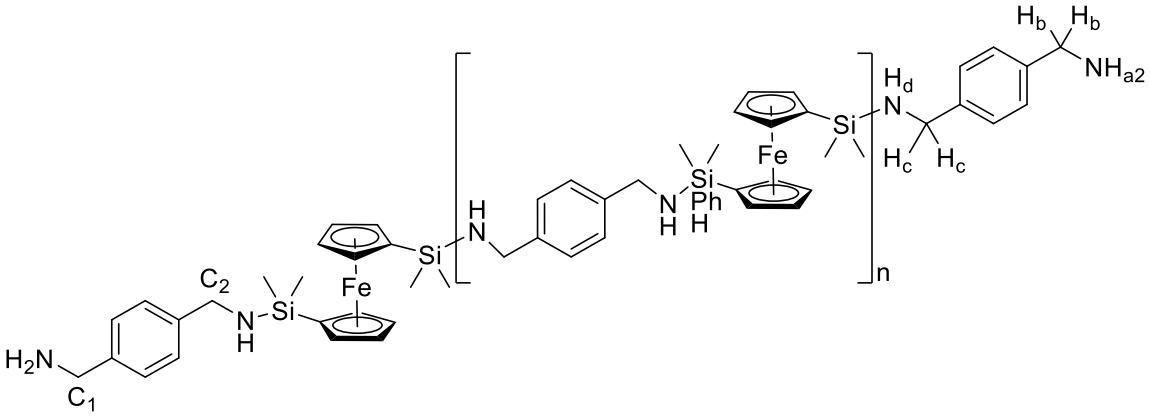

Synthesis of polymer P14. In the glove box, 0.210 g compound **1** (0.72 mmol) and 0.098 g *p*-xylylenediamine (0.72 mmol) were dissolved in 1 ml THF in a Schlenk flask. 14.3 mg compound **III** (0.024 mmol) was dissolved in 0.1 ml THF, and added to the stirred monomer solution, resulting in an immediate colour change to purple, and vigorous bubbling. The reaction was stirred for 45 minutes, then 17.8 µl $PhSiH_3$ (0.144 mmol) was added. The reaction mixture resumed bubbling and rapidly increased in viscosity, becoming a gelatinous lump after a few seconds. The bubbling subsided, and the Schlenk flask was removed from the box. Most of the solvent was removed under vacuum, before backfilling with air in order to quench the catalyst and purple colour. The product was isolated as a spongy orange solid following prolonged vacuum drying. Addition of solvent (benzene, toluene, or THF) resulted only in swelling to an orange gel, precluding characterisation by NMR spectroscopy. A small amount of soluble material could be extracted from the gel with C_6D_6. The ^{1}H NMR spectrum of this extract resembled that of polymers **P1-P7**, assumed to be a fraction of polymer which was not crosslinked by addition of phenylsilane. A pellet of **P14** could be obtained by compressing a 30 mg sample of the polymer in a KBr press in the glove box.

X-ray Crystallography

Data for compound **1** were collected on an Agilent Xcalibur, diffractometer equipped with a Mo-Ka source while those for compounds **2**-**8** were collected on a SuperNova machine using Cu-K□ radiation. All samples were maintained at 150 K during data collection. Using Olex2,[134] all structures were solved with the olex2.solve[134] structure solution program and subsequently refined using the SHELXL[135] program. While refinements were largely unremarkable, there are some points which merit note as follows: For compounds **1** and **6**, H1A and H1B, attached to Si1, were located and refined without restraints. For compounds **2**, **4**, **5** and **7**, nitrogen bound hydrogen atoms were located and refined at a distance of 0.98 Å from the relevant parent atom.

The asymmetric unit of **4** comprises half of a molecule in which the transition metal is coincident with a crystallographic inversion centre. The structure of **5** is a textbook presentation of 'almost but not quite' in terms of symmetry, being metrically close to a monoclinic *C* unit cell. However, the latter was not supported, even by invoking a twin law. Ultimately, the crystal was single, and the solution was brokered, as presented here, in space group *P*-1.

The integration of the raw data for **8** took account of the fact that the sample was a two component twin (53:47 ratio), by virtue of a 180° rotation about the *c* axis. Half of one molecule was seen to comprise the asymmetric unit, the remainder being generated *via* an inversion centre intrinsic to the space group. H1 was located and refined without restraints.

Crystallographic data for all compounds have been deposited with the Cambridge Crystallographic Data Centre as supplementary publications CCDC 1937585-1937592 for compounds **1**-**8**, respectively. Copies of these data can be obtained free of charge on application to CCDC, 12 Union Road, Cambridge CB2 1EZ, UK [fax(+44) 1223 336033, e-mail: deposit@ccdc.cam.ac.uk.

Supporting Information

Supporting Information is available free of charge on the ACS Publications website at DOI:

X-ray crystal structures of compounds **1**, **3**, **6**, and **8**, X-ray crystallographic details, additional ceramic characterisation data, differential scanning calorimetry, additional thermogravimetric analysis, NMR spectra and DOSY plots for compounds and polymers, additional cyclic voltammetry data.

Acknowledgements

We acknowledge financial support from the EPSRC Centre for Doctoral Training in Catalysis (EP/L016443/1) and Dr John Lowe (University of Bath) for his assistance with DOSY

experiments. IM thanks the University of Bristol for support and the Canadian Government for a C150 Research Chair.

Statement about conflict of interests

The authors declare no competing financial interests.

References

1. Jiang, X.; Li, R. R.; Feng, C.; Lu, G. L.; Huang, X. Y., Triple-stimuli-responsive ferrocene-containing homopolymers by RAFT polymerization. *Polymer Chem.***2017,** *8* (18), 2773-2784.
2. Yang, P.; Pageni, P.; Kabir, M. P.; Zhu, T.; Tang, C., Metallocene-Containing Homopolymers and Heterobimetallic Block Copolymers via Photoinduced RAFT Polymerization. *ACS Macro Lett.***2016,** *5*, 1293-1300.
3. Manners, I., Ring-opening polymerization (ROP) of strained, ring-tilted silicon-bridged [1]ferrocenophanes: Synthetic methods and mechanisms. *Polyhedron* **1996,** *15*, 4311-4329.
4. Whittell, G. R.; Manners, I., Metallopolymers: New multifunctional materials. *Adv. Mater.* **2007,** *19*, 3439-3468.
5. Neuse, E.; Rosenberg, H., Metallocene Polymers. *Polymer Rev.* **1970,** *4*, 1-145.
6. Neuse, E. W.; Bednarik, L., Metallocene Polymers .37. Organolithium organo-halide coupling reaction as a synthetic route to poly(1,1'-ferrocenylenes). *Macromolecules* **1979,** *12* (2), 187-195.
7. Ho, C.-L.; Yu, Z.-Q.; Wong, W.-Y., Multifunctional polymetallaynes: properties, functions and applications. *Chem. Soc. Rev.* **2016,** *45*, 5264-5295.
8. Zhang, K. Y.; Liu, S.; Zhao, Q.; Huang, W., Stimuli-responsive metallopolymers. *Coord. Chem. Rev.* **2016,** *319*, 180-195.
9. Jaska, C. A.; Bartole-Scott, A.; Manners, I., Metal-catalyzed routes to rings, chains and macromolecules based on inorganic elements. *Dalton Trans.***2003,** (21), 4015--4021.
10. Whittell, G. R.; Hager, M. D.; Schubert, U. S.; Manners, I., Functional soft materials from metallopolymers and metallosupramolecular polymers. *Nature Mater.* **2011,** *10*, 176-188.
11. Alkan, A. a. G. T. a. W. F. R., Ruthenocenyl Glycidyl Ether: A Ruthenium-Containing Epoxide for Anionic Polymerization. *Organometallics* **2017,** *36* (16), 3023--3028.
12. Alkan, A.; Wurm, F. R., Water-Soluble Metallocene-Containing Polymers. *Macromolecular Rapid Commun.* **2016,** *37* (18), 1482-1493.
13. Zoetebier, B.; Sohrabi, A.; Lou, B.; Hempenius, M. A.; Hennink, W. E.; Vancso, G. J., PEG stabilized DNA - poly(ferrocenylsilane) polyplexes for gene delivery. *Chem. Commun.* **2016,** *52*, 7707-7710.
14. Feng, X.; Zhang, K.; Hempenius, M. A.; Vancso, G. J., Organometallic polymers for electrode decoration in sensing applications. *RSC Adv.* **2015,** *5* (129), 106355-106376.
15. Hempenius, M. A.; Cirmi, C.; Lo Savio, F.; Song, J.; Vancso, G. J., Poly(ferrocenylsilane) Gels and Hydrogels with Redox-Controlled Actuation. *Macromolecular Rapid Commun.* **2010,** *31* (9-10), 772-783.
16. Gallei, M.; Ruttiger, C., Recent Trends in Metallopolymer Design: Redox-Controlled Surfaces, Porous Membranes, and Switchable Optical Materials Using Ferrocene-Containing Polymers. *Chem. Eur. J.* **2018,** *24* (40), 10006-10021.
17. Ruttiger, C.; Hubner, H.; Schottner, S.; Winter, T.; Cherkashinin, G.; Kuttich, B.; Stuhn, B.; Gallei, M., Metallopolymer-Based Block Copolymers for the Preparation of Porous and Redox-Responsive Materials. *ACS Appl. Mater. & Interfaces* **2018,** *10* (4), 4018-4030.
18. Elbert, J.; Didzoleit, H.; Fasel, C.; Ionescu, E.; Riedel, R.; Stuhn, B.; Gallei, M., Surface-initiated anionic polymerization of [1]silaferrocenophanes for the preparation of colloidal preceramic materials. *Macromolecular Rapid Commun.* **2015,** *36* (7), 597-603.
19. Foucher, D. a.; Tang, B.-Z.; Manners, I., Ring-opening polymerization of strained, ring-tilted ferrocenophanes: a route to high-molecular-weight poly (ferrocenylsilanes). *J. Am. Chem. Soc.* **1992,** *114*, 6246-6248.
20. Hailes, R. L. N.; Oliver, A. M.; Gwyther, J.; Whittell, G. R.; Manners, I., Polyferrocenylsilanes: Synthesis, properties, and applications. *Chem. Soc. Rev.* **2016,** *45* (19), 5358--5407.
21. Peckham, T. J.; Massey, J. A.; Honeyman, C. H.; Manners, I., Living anionic polymerization of phosphorus-bridged 1 ferrocenophanes: Synthesis and characterization of well-defined poly(ferrocenylphosphine) homopolymers and block copolymers. *Macromolecules* **1999,** *32* (9), 2830-2837.
22. Sarbisheh, E. K.; Flores, J. E.; Zhu, J. F.; Muller, J., Insight into the Thermal Ring-Opening Polymerization of Phospha 1 ferrocenophanes. *Chem. Eur. J.* **2016,** *22* (47), 16836-16847.
23. Jakle, F.; Vidal, F., Functional Polymeric Materials Based on Main-Group Elements. *Angewandte Chemie-International Edition* **2019,** *58*, 5846-5870.
24. Flory, P. J., Molecular Size Distribution in Linear Condensation Polymers '. *J. Am. Chem. Soc.* **1936,** *58* (7), 1877--1885.

25. Carothers, W. H., Polymers and polyfunctionality. *Trans. Faraday Soc.* **1936,** *32*, 39-49.
26. Kucinski, K.; Hreczycho, G., Catalytic Formation of Silicon-Heteroatom (N, P, O, S) Bonds. *Chemcatchem* **2017,** *9* (11), 1868-1885.
27. Gauvin, F.; Harrod, J. F.; Woo, H. G., Catalytic dehydrocoupling: A general strategy for the formation of element-element bonds. *Adv. Organometal. Chem., Vol 42* **1998,** *42*, 363-405.
28. Leitao, E. M.; Jurca, T.; Manners, I., Catalysis in service of main group chemistry offers a versatile approach to p-block molecules and materials. *Nature Chem.* **2013,** *5*, 817-29.
29. Waterman, R., Mechanisms of metal-catalyzed dehydrocoupling reactions. *Chem. Soc. Rev.* **2013,** *42* (13), 5629-5641.
30. Priegert, A. M.; Rawe, B. W.; Serin, S. C.; Gates, D. P., Polymers and the p-block elements. *Chem. Soc. Rev.* **2016,** *45* (4), 922-953.
31. Clark, T. J.; Lee, K.; Manners, I., Transition-metal-catalyzed dehydrocoupling: A convenient route to bonds between main-group elements. *Chem. Eur. J.* **2006,** *12*, 8634-8648.
32. Kim, B. H.; Cho, M. S.; Woo, H. G., Si-Si/Si-C/Si-O/Si-N coupling of hydrosilanes to useful silicon-containing materials. *Synlett* **2004,** (5), 761-772.
33. McWilliams, A. R.; Dorn, H.; Manners, I., New inorganic polymers containing phosphorus. *New Aspects in Phosphorus Chemistry I* **2002,** *220*, 141-167.
34. Corey, J. Y., Dehydrocoupling of Hydrosilanes to Polysilanes and Silicon Oligomers: A 30 Year Overview. *Adv. Organometal. Chem.* **2004,** *51* (1), 1--52.
35. Smith, E. E.; Du, G. D.; Fanwick, P. E.; Abu-Omar, M. M., Dehydrocoupling of Organosilanes with a Dinuclear Nickel Hydride Catalyst and Isolation of a Nickel Silyl Complex. *Organometallics* **2010,** *29* (23), 6527-6533.
36. Kim, B. H.; Cho, M. S.; Kim, M. A.; Woo, G. G., One-pot synthesis of poly(alkoxysilane)s by Si-Si/Si-O dehydrocoupling of silanes with alcohols using Group IV and VIII metallocene complexes. *J. Organometal. Chem.* **2003,** *685*, 93-98.
37. Caseri, W., Polystannanes: processible molecular metals with defined chemical structures. *Chem. Soc. Rev.* **2016,** *45* (19), 5187-5199.
38. Braunstein, P.; Morise, X., Dehydrogenative coupling of hydrostannanes catalyzed by transition-metal complexes. *Chem. Rev.***2000,** *100* (10), 3541-3552.
39. Imori, T.; Tilley, T. D., High-molecular-mass polystannanes via dehydropolymerization of di(n-butyl)stannane. *J. Chem. Soc.-Chem. Commun.* **1993,** (21), 1607-1609.
40. Trummer, M.; Choffat, F.; Smith, P.; Caseri, W., Polystannanes: Synthesis, Properties, and Outlook. *Macromolecular Rapid Commun.* **2012,** *33* (6-7), 448-460.
41. Staubitz, A.; Sloan, M. E.; Robertson, A. P. M.; Friedrich, A.; Schneider, S.; Gates, P. J.; Manners, I.; Schmedt auf der Guenne, J., Catalytic Dehydrocoupling / Dehydrogenation of N-Methylamine-Borane and Ammonia-Borane : Synthesis and Characterization of High Molecular Weight Polyaminoboranes. *J. Am. Chem. Soc.* **2010,** *132*, 13332-13345.
42. Coles, N. T.; Mahon, M. F.; Webster, R. L., Phosphine- and Amine-Borane Dehydrocoupling Using a Three-Coordinate Iron(II) beta-Diketiminate Precatalyst. *Organometallics* **2017,** *36* (11), 2262-2268.
43. Webster, R. L., β-Diketiminate complexes of the first row transition metals: applications in catalysis. *Dalton Trans.* **2017**.
44. Staubitz, A.; Soto, A. P.; Manners, I., Iridium-catalyzed dehydrocoupling of primary amine-borane adducts: A route to high molecular weight polyaminoboranes, boron-nitrogen analogues of polyolefins. *Angew. Chem. Int. Ed.***2008,** *47* (33), 6212-6215.
45. Vance, J. R.; Schafer, A.; Robertson, A. P. M.; Lee, K.; Turner, J.; Whittell, G. R.; Manners, I., Iron-Catalyzed Dehydrocoupling/Dehydrogenation of Amine-Boranes. *J. Am. Chem. Soc.* **2014,** *136* (8), 3048-3064.
46. Marquardt, C.; Jurca, T.; Schwan, K. C.; Stauber, A.; Virovets, A. V.; Whittell, G. R.; Manners, I.; Scheer, M., Metal-Free Addition/Head-to-Tail Polymerization of Transient Phosphinoboranes, RPH-BH2: A Route to Poly(alkylphosphinoboranes). *Angew. Chem. Int. Ed.***2015,** *54* (46), 13782-13786.
47. Schäfer, A.; Jurca, T.; Turner, J.; Vance, J. R.; Lee, K.; Du, V. A.; Haddow, M. F.; Whittell, G. R.; Manners, I., Iron-catalyzed dehydropolymerization: A convenient route to poly(phosphinoboranes) with molecular-weight control. *Angew. Chem. Int. Ed.* **2015,** *54*, 4836-4841.
48. Paul, U. S. D.; Braunschweig, H.; Radius, U., Iridium-catalysed dehydrocoupling of aryl phosphine-borane adducts: synthesis and characterisation of high molecular weight poly(phosphinoboranes). *Chem. Commun.* **2016,** *52* (55), 8573-8576.
49. Turner, J. R.; Resendiz-Lara, D. A.; Jurca, T.; Schäfer, A.; Vance, J. R.; Beckett, L.; Whittell, G. R.; Musgrave, R. A.; Sparkes, H. A.; Manners, I., Synthesis, Characterization, and Properties of Poly(aryl)phosphinoboranes Formed via Iron-Catalyzed Dehydropolymerization. *Macromolecular Chem. and Phys.* **2017,** *1700120*, 1700120.
50. Dorn, H.; Singh, R. A.; Massey, J. A.; Nelson, J. M.; Jaska, C. A.; Lough, A. J.; Manners, I., Transition metal-catalyzed formation of phosphorus-boron bonds a new route to phosphinoborane rings, chains, and macromolecules. *J. Am. Chem. Soc.* **2000,** *122*, 6669-6678.
51. Dorn, H.; Manners, I., Transition metal-catalyzed formation of phosphorus-boron bonds: a new route to phosphinoborane rings, chains and the first high polymers. *Phosphorus Sulfur and Silicon and the Related Elements* **2001,** *168*, 185-190.

52. Yamaguchi, I.; Ishii, H.; Sakano, T.; Osakada, K.; Yamamoto, T., Rhodium- and ruthenium-complex-catalyzed condensation of ferrocene-containing dithiols and diols with diarylsilanes to give silaferrocenophanes and ferrocene polymers. *Appl. Organometal. Chem.* **2001,** *15*, 197-203.
53. Pandey, S.; Lonnecke, P.; Hey-Hawkins, E., Phosphorus-Boron-Based Polymers Obtained by Dehydrocoupling of Ferrocenylphosphine- Borane Adducts. *Eur. J. Inorg. Chem.* **2014,** *2014* (14), 2456-2465.
54. Fessenden, R.; Fessenden, J. S., The chemistry of silicon-nitrogen compounds. *Chem. Rev.***1961,** *61* (4), 361-388.
55. Passarelli, V.; Carta, G.; Rossetto, G.; Zanella, P., Aminolysis of the Si-Cl bond and ligand exchange reaction between silicon amido derivatives and $SiCl_4$: synthetic applications and kinetic investigations. *Dalton Trans.***2003,** (3), 413-419.
56. Tanabe, Y.; Murakami, M.; Kitaichi, K.; Yoshida, Y., Mild, effective and selective method for the silylation of alcohols using silazanes promoted by catalytic tetrabutylammonium fluoride. *Tetrahedron Lett.* **1994,** *35* (45), 8409-8412.
57. Tanabe, Y.; Misaki, T.; Kurihara, M.; Iida, A.; Nishii, Y., Silazanes/catalytic bases: mild, powerful and chemoselective agents for the preparation of enol silyl ethers from ketones and aldehydes. *Chem. Commun.* **2002,** (15), 1628-1629.
58. Lenhart, S. J.; Blum, Y. D.; Laine, R. M., The corrosion-resistance of an aluminum-alloy coated with polysilazane-derived ceramics. *Corrosion* **1989,** *45* (6), 503-506.
59. Corriu, R. J. P.; Leclercq, D.; Mutin, P. H.; Planeix, J. M.; Vioux, A., Silicon-nitrogen bond formation by nucleophilic activation of silicon hydrogen-bonds. *J. Organometal. Chem.* **1991,** *406* (1-2), C1-C4.
60. Birot, M.; Pillot, J. P.; Dunogues, J., Comprehensive chemistry of polycarbosilanes, polysilazanes, and polycarbosilazanes as precursors of ceramics. *Chem. Rev.***1995,** *95* (5), 1443-1477.
61. Kroke, E.; Li, Y. L.; Konetschny, C.; Lecomte, E.; Fasel, C.; Riedel, R., Silazane derived ceramics and related materials. *Mater. Sci. & Eng. Reports* **2000,** *26* (4-6), 97-199.
62. Blum, Y. D.; Schwartz, K. B.; Laine, R. M., preceramic polymer pyrolysis .1. Pyrolytic properties of polysilazanes. *J. Mater. Sci.* **1989,** *24* (5), 1707-1718.
63. Bernard, A. S.; Viard, A.; Fonblanc, D.; Lale, A.; Salameh, C.; Wynn, M.; Champagne, P.; Babonneau, F.; Chollon, G.; Gervais, C.; Viard, A.; Fonblanc, D.; Schmidt, M.; Lale, A.; Salameh, C., Molecular Chemistry and Engineering of Boron-Modified Polyorganosilazanes as New Processable and Functional SiBCN Precursors. *Chem. Eur. J.* **2017,** *23* (38), 9076-9090.
64. Xie, W. L.; Hu, H. F.; Cui, C. M., (NHC)Yb{$N(SiMe_3)_2$}$_2$ -Catalyzed Cross-Dehydrogenative Coupling of Silanes with Amines. *Angew. Chem. Int. Ed.***2012,** *51* (44), 11141-11144.
65. Nako, A. E.; Chen, W. Y.; White, A. J. P.; Crimmin, M. R., Yttrium-Catalyzed Amine-Silane Dehydrocoupling: Extended Reaction Scope with a Phosphorus-Based Ligand. *Organometallics* **2015,** *34* (17), 4369-4375.
66. Li, N.; Guan, B. T., Yttrium-Benzyl Complexes Bearing Chiral Iminophosphonamide Ligands: Synthesis and Application in Catalytic Asymmetric Amine-Silane Dehydrocoupling Reactions. *Adv. Synth. & Catal.* **2017,** *359* (20), 3526-3531.
67. Pindwal, A.; Ellern, A.; Sadow, A. D., Homoleptic Divalent Dialkyl Lanthanide-Catalyzed Cross-Dehydrocoupling of Silanes and Amines. *Organometallics* **2016,** *35* (11), 1674-1683.
68. Wang, J. X.; Dash, A. K.; Berthet, J. C.; Ephritikhine, M.; Eisen, M. S., Dehydrocoupling reactions of amines with silanes catalyzed by $(Et_2N)_3U$ BPh_4. *J. Organometal. Chem.* **2000,** *610* (1-2), 49-57.
69. Rios, P.; Rosello-Merino, M.; Rivada-Wheelagham, O.; Borge, J.; Lopez-Serrano, J.; Conejero, S., Selective catalytic synthesis of amino-silanes at part-per million catalyst loadings. *Chem. Commun.* **2018**.
70. Konigs, C. D. F.; Muller, M. F.; Aiguabella, N.; Klare, H. F. T.; Oestreich, M., Catalytic dehydrogenative Si-N coupling of pyrroles, indoles, carbazoles as well as anilines with hydrosilanes without added base. *Chem. Commun.* **2013,** *49* (15), 1506-1508.
71. Wang, W. D.; Eisenberg, R., Dehydrogenative coupling reactions to form silazane oligomers promoted by binuclear rhodium complexes. *Organometallics* **1991,** *10* (7), 2222-2227.
72. Liu, H. Q.; Harrod, J. F., Copper(I)-catalyzed cross-dehydrocoupling reactions of silanes and amines. *Canad. J. Chem.-Revue Can. Chim.* **1992,** *70* (1), 107-110.
73. Liu, H. Q.; Harrod, J. F., Dehydrocoupling of ammonia and silanes catalyzed by dimethyltitanocene. *Organometallics* **1992,** *11* (2), 822-827.
74. Anga, S.; Sarazin, Y.; Carpentier, J. F.; Panda, T. K., Alkali-Metal-Catalyzed Cross-Dehydrogenative Couplings of Hydrosilanes with Amines. *Chemcatchem* **2016,** *8* (7), 1373-1378.
75. Greb, L.; Tamke, S.; Paradies, J., Catalytic metal-free Si-N cross-dehydrocoupling. *Chem. Commun.* **2014,** *50* (18), 2318-2320.
76. Allen, L. K.; Garcia-Rodriguez, R.; Wright, D. S., Stoichiometric and catalytic Si-N bond formation using the p-block base Al(NMe2)(3). *Dalton Trans.***2015,** *44* (27), 12112-12118.
77. Blandez, J. F.; Esteve-Adell, I.; Alvaro, M.; Garcia, H., Palladium nanoparticles supported on graphene as catalysts for the dehydrogenative coupling of hydrosilanes and amines. *Catal. Sci. & Tech.* **2015,** *5* (4), 2167-2173.
78. Mitsudome, T.; Urayama, T.; Maeno, Z.; Mizugaki, T.; Jitsukawa, K.; Kaneda, K., Highly Efficient Dehydrogenative Coupling of Hydrosilanes with Amines or Amides Using Supported Gold Nanoparticles. *Chem. Eur. J.* **2015,** *21* (8), 3202-3205.

79. Buch, F.; Harder, S., The Azametallacyclopropane Ca (η 2 -Ph 2 CNPh)(hmpa) 3 : A Calcium Alternative to a Versatile Ytterbium (II) Catalyst. *Organometallics* **2007,** *26*, 5132-5135.
80. Dunne, J. F.; Neal, S. R.; Engelkemier, J.; Ellern, A.; Sadow, A. D., Tris(oxazolinyl)boratomagnesium-catalyzed cross-dehydrocoupling of organosilanes with amines, hydrazine, and ammonia. *J. Am. Chem. Soc.* **2011,** *133*, 16782-16785.
81. Baishya, A.; Peddarao, T.; Nembenna, S., Organomagnesium amide catalyzed crossdehydrocoupling of organosilanes with amines. *Dalton Trans.***2017,** *46* (18), 5880-5887.
82. Hill, M. S.; Liptrot, D. J.; MacDougall, D. J.; Mahon, M. F.; Robinson, T. P., Hetero-dehydrocoupling of silanes and amines by heavier alkaline earth catalysis. *Chem. Sci.***2013,** *4* (11), 4212.
83. Bellini, C.; Orione, C.; Carpentier, J. F.; Sarazin, Y., Tailored Cyclic and Linear Polycarbosilazanes by Barium-Catalyzed N-H/H-Si Dehydrocoupling Reactions. *Angew. Chem. Int. Ed.* **2016,** *55*, 3744-3748.
84. Bellini, C.; Roisnel, T.; Carpentier, J. F.; Tobisch, S.; Sarazin, Y., Sequential Barium-Catalysed N-H/H-Si Dehydrogenative Cross-Couplings: Cyclodisilazanes versus Linear Oligosilazanes. *Chem. Eur. J.* **2016,** *22*, 15733-15743.
85. Bellini, C.; Dorcet, V.; Carpentier, J. F.; Tobisch, S.; Sarazin, Y., Alkaline-Earth-Catalysed Cross-Dehydrocoupling of Amines and Hydrosilanes: Reactivity Trends, Scope and Mechanism. *Chem. Eur. J.* **2016,** *22*, 4564-4583.
86. Bellini, C.; Carpentier, J.-F.; Tobisch, S.; Sarazin, Y., Barium-Mediated Cross-Dehydrocoupling of Hydrosilanes with Amines: A Theoretical and Experimental Approach. *Angew. Chem. Int. Ed.* **2015,** *54*, 7679-7683.
87. Li, W.; Chung, H.; Daeffler, C.; Johnson, J. A.; Grubbs, R. H., Application of 1H DOSY for facile measurement of polymer molecular weights. *Macromolecules* **2012,** *45*, 9595-9603.
88. Wrackmeyer, B.; Klimkina, E. V.; Milius, W., 1,3-Bis(trimethylsilyl)-1,3,2-diazaphospha- 3 ferrocenophanes. *Z. Anorg. Allg. Chem.* **2010,** *636* (5), 784-794.
89. Bhattacharjee, H.; Dey, S.; Zhu, J. F.; Sun, W.; Muller, J., Strained azabora 2 ferrocenophanes. *Chem. Commun.* **2018,** *54* (44), 5562-5565.
90. Auch, T. C.; Braunschweig, H.; Radacki, K.; Sigritz, R.; Siemeling, U.; Stellwag, S., Synthesis and crystal structure of 1,3-diphenyl-2-ferrocenyl-1,3,2-diazabora- 3 ferrocenophane. *Z. Naturforsch. Sect. B - J. Chem. Sci.* **2008,** *63* (7), 920-922.
91. Walz, F.; Moos, E.; Garnier, D.; Koppe, R.; Anson, C. E.; Breher, F., A Redox-Switchable Germylene and its Ligating Properties in Selected Transition Metal Complexes. *Chem. Eur. J.* **2017,** *23* (5), 1173-1186.
92. Oetzel, J.; Weyer, N.; Bruhn, C.; Leibold, M.; Gerke, B.; Pottgen, R.; Maier, M.; Winter, R. F.; Holthausen, M. C.; Siemeling, U., Redox-Active N-Heterocyclic Germylenes and Stannylenes with a Ferrocene-1,1 '-diyl Backbone. *Chem. Eur. J.* **2017,** *23* (5), 1187-1199.
93. Moser, C.; Belaj, F.; Pietschnig, R., Phosphorus-Rich Ferrocenophanes. *Phosphorus Sulfur and Silicon and the Related Elements* **2015,** *190* (5-6), 837-844.
94. Wrackmeyer, B.; Klimkina, E. V.; Milius, W., 1,3,2-Diazaphospha- 3 ferrocenophanes. Molecular Structures and Multinuclear Magnetic Resonance Studies. *Z. Naturforsch. Sect. B - J. Chem. Sci.* **2009,** *64* (11-12), 1401-1412.
95. Wrackmeyer, B.; Klimkina, E. V.; Milius, W., 1,3,2-diazaalumina- 3 ferrocenophanes with alkyn-1-yl substituents at aluminum. *Z. Naturforsch. Sect. B - J. Chem. Sci.* **2007,** *62* (10), 1259-1266.
96. Wrackmeyer, B.; Klimkina, E. V.; Milius, W., Ferrocenophanes with interannular nitrogen-aluminum bridges - Synthesis and structure. *Z. Anorg. Allg. Chem.* **2007,** *633* (11-12), 1964-1972.
97. Wrackmeyer, B.; Klimkina, E. V.; Milius, W., Novel diaminoaluminum halides and a diaminoaluminum hydride: 1,3,2-Diazaalumina- 3 ferrocenophanes. *Polyhedron* **2007,** *26* (14), 3496-3504.
98. Wrackmeyer, B.; Klimkina, E. V.; Milius, W., Spiro compounds of tin, selenium and tellurium containing 1,3,2-diazaelement- 3 ferrocenophane units. *Z. Anorg. Allg. Chem.* **2006,** *632* (14), 2331-2340.
99. Wrackmeyer, B.; Klunkina, E. V.; Millus, W.; Tok, O. L.; Herberhold, M., Novel 1,3,2-diazabora- 3 ferrocenophanes and a 1,4,2,3-diazadibora- 4 ferrocenophane. *Inorg. Chim. Acta* **2005,** *358* (5), 1420-1428.
100. Wrackmeyer, B.; Klimkina, E. V.; Milius, W., The first 1,3,2-diazaphospha- 3 ferrocenophanes. *Inorg. Chem. Commun.* **2004,** *7* (7), 884-888.
101. Wrackmeyer, B.; Klimkina, E. V.; Milius, W., A novel 6 ferrocenophane containing a N-Si-C-C-Si-N bridge, in equilibrium by ring-opening with an 1,1 '-diaminoferrocene derivative. *Inorg. Chem. Commun.* **2004,** *7* (3), 412-416.
102. Wrackmeyer, B.; Klimkina, E. V.; Maisel, H. E.; Milius, W.; Herberhold, M., The first 1,3,2-diazabora-3 ferrocenophanes - molecular structures and dynamic behaviour in solution. *Inorg. Chim. Acta* **2004,** *357* (6), 1703-1710.
103. Musgrave, R. A.; Russell, A. D.; Manners, I., Strained ferrocenophanes. *Organometallics* **2013,** *32* (20), 5654-5667.
104. Hailes, R.; Musgrave, R. A.; Kilpatrick, A. F. R.; Russell, A. D.; Whittell, G. R.; O'Hare, D.; Manners, I., Ring-Opening Polymerisation of Low-Strain Nickelocenophanes: Synthesis and Magnetic Properties of Polynickelocenes with Carbon and Silicon Main Chain Spacers. *Chem. Eur. J.* **2019,** *25* (4), 1044-1054.
105. Russell, A. D.; Musgrave, R. A.; Stoll, L. K.; Choi, P.; Qiu, H.; Manners, I., Recent developments with strained metallocenophanes. *J. Organometal. Chem.* **2015,** *784*, 24-30.

106. Musgrave, R. A.; Russell, A. D.; Hayward, D. W.; Whittell, G. R.; Lawrence, P. G.; Gates, P. J.; Green, J. C.; Manners, I., Main-chain metallopolymers at the static–dynamic boundary based on nickelocene. *Nature Chem.* **2017**, *9*, 743–750.
107. Corriu, R. J. P.; Devylder, N.; Guerin, C.; Henner, B.; Jean, A., Oligomers with silicon, germanium, and transition-metal groups - synthesis and characterization of metal-containing poly (silylene)diacetylenes and poly (germylene)diacetylenes. *Organometallics* **1994,** *13* (8), 3194-3202.
108. Jain, R.; Choi, H.; Lalancette, R. A.; Sheridan, J. B., Bi- and triferrocene complexes containing silylenevinylenephenylene bridges. Model compounds for poly{ferrocene(phenylene)bis(silylenevinylene)}s. *Organometallics* **2005,** *24*, 1468-1476.
109. Schottner, S.; Hossain, R.; Ruttiger, C.; Gallei, M., Ferrocene-Modified Block Copolymers for the Preparation of Smart Porous Membranes. *Polymers* **2017,** *9* (10), 491.
110. Zhang, K. H.; Zhang, M. M.; Feng, X. L.; Hempenius, M. A.; Vancso, G. J., Switching Light Transmittance by Responsive Organometallic Poly(ionic liquid)s: Control by Cross Talk of Thermal and Redox Stimuli. *Adv. Funct. Mater.* **2017,** *27* (41), 1702784.
111. Fisher, A. C., *Electrode Dynamics*. Oxford University Press: Oxford, 1996.
112. Wilke, C. R.; Chang, P., Correlation of diffusion coefficients in dilute solutions. *AIChE Journal* **1955,** *1* (2), 264-270.
113. Flanagan, J. B.; Margel, S.; Bard, A. J.; Anson, F. C., Electron-transfer to and from molecules containing multiple, noninteracting redox centers - electrochemical oxidation of poly(vinylferrocene). *J. Am. Chem. Soc.* **1978,** *100* (13), 4248-4253.
114. Petersen, R.; Foucher, D. A.; Tang, B. Z.; Lough, A.; Raju, N. P.; Greedan, J. E.; Manners, I., Pyrolysis of poly(ferrocenylsilanes) - synthesis and characterization of ferromagnetic transition metal-containing ceramics and molecular depolymerization products. *Chem. Mater.* **1995,** *7* (11), 2045-2053.
115. Ginzburg, M.; MacLachlan, M. J.; Yang, S. M.; Coombs, N.; Coyle, T. W.; Raju, N. P.; Greedan, J. E.; Herber, R. H.; Ozin, G. A.; Manners, I., Genesis of nanostructured, magnetically tunable ceramics from the pyrolysis of cross-linked polyferrocenylsilane networks and formation of shaped macroscopic objects and micron scale patterns by micromolding inside silicon wafers. *J. Am. Chem. Soc.* **2002,** *124* (11), 2625-2639.
116. Liu, K.; Clendenning, S. B.; Friebe, L.; Chan, W. Y.; Zhu, X. B.; Freeman, M. R.; Yang, G. C.; Yip, C. M.; Grozea, D.; Lu, Z. H.; Manners, I., Pyrolysis of highly metallized polymers: Ceramic thin films containing magnetic CoFe alloy nanoparticles from a polyferrocenylsilane with pendant cobalt clusters. *Chem. Mater.* **2006,** *18* (10), 2591-2601.
117. MacLachlan, M. J.; Ginzburg, M.; Coombs, N.; Coyle, T. W.; Raju, N. P.; Greedan, J. E.; Ozin, G. A.; Manners, I., Shaped ceramics with tunable magnetic properties from metal-containing polymers. *Science* **2000,** *287* (5457), 1460-1463.
118. Kulbaba, K.; Cheng, A.; Bartole, A.; Greenberg, S.; Resendes, R.; Coombs, N.; Safa-Sefat, A.; Greedan, J. E.; Stover, H. D. H.; Ozin, G. A.; Manners, I., Polyferrocenylsilane microspheres: Synthesis, mechanism of formation, size and charge tunability, electrostatic self-assembly, and pyrolysis to spherical magnetic ceramic particles. *J. Am. Chem. Soc.* **2002,** *124* (42), 12522-12534.
119. Galloro, J.; Ginzburg, M.; Miguez, H.; Yang, S. M.; Coombs, N.; Safa-Sefat, A.; Greedan, J. E.; Manners, I.; Ozin, G. A., Replicating the structure of a crosslinked polyferrocenylsilane inverse opal in the form of a magnetic ceramic. *Adv. Funct. Mater.* **2002,** *12* (5), 382-388.
120. Liu, K.; Fournier-Bidoz, S.; Ozin, G. A.; Manners, I., Highly Ordered Magnetic Ceramic Nanorod Arrays from a Polyferrocenylsilane by Nanoimprint Lithography with Anodic Aluminum Oxide Templates. *Chemistry of Materials* **2009,** *21* (9), 1781-1783.
121. Tang, B. Z.; Petersen, R.; Foucher, D. A.; Lough, A.; Coombs, N.; Sodhi, R.; Manners, I., Novel ceramic and organometallic depolymerization products from poly(ferrocenylsilanes) via pyrolysis. *J. Chem. Soc.-Chem. Commun.* **1993,** (6), 523-525.
122. Hanawalt, J. D.; Rinn, H. W.; Frevel, L. K., Chemical Analysis by X-Ray Diffraction. *Ind. Eng. Chem. Anal. Ed.* **1938,** *10* (9), 457-512.
123. Morris, M. C.; McMurdie, H. F.; Evans, E. H.; Paretzkin, B.; Parker, H. S.; Panagiotopoulos, N. C.; Hubbard, C. R., Standard X-ray Diffraction Powder Patterns. In *National Bureau of Standards (U.S.) Monograph 25*, 1981; Vol. 18, p 37.
124. Leslie-Pelecky, D. L.; Rieke, R. D., Magnetic properties of nanostructured materials. *Chem. Mater.* **1996,** *8* (8), 1770-1783.
125. Stevens, J. R.; Plieger, P. G., Anion-driven conformation control and enhanced sulfate binding utilising aryl linked salicylaldoxime dicopper helicates. *Dalton Trans.***2011,** *40*, 12235.
126. Westerhausen, M., Synthesis and spectroscopic properties of bis(trimethylsilyl)amides of the alkaline-earth metals magnesium, calcium, strontium, and barium. *Inorg. Chem.* **1991,** *30*, 96-101.
127. Sarazin, Y.; Howard, R. H.; Hughes, D. L.; Humphrey, S. M.; Bochmann, M., Titanium, zinc and alkaline-earth metal complexes supported by bulky *O,N,N,O*-multidentate ligands: syntheses, characterisation and activity in cyclic ester polymerisation. *Dalton Trans.***2006,** (2), 340-350.
128. Wixey, J. S.; Ward, B. D., Modular ligand variation in calcium bisimidazoline complexes: effects on ligand redistribution and hydroamination catalysis. *Dalton Trans.***2011,** *40* (30), 7693-7696.
129. Crimmin, M. R.; Barrett, A. G. M.; Hill, M. S.; MacDougall, D. J.; Mahon, M. F.; Procopiou, P. A., Bis(trimethylsilyl)methyl derivatives of calcium, strontium and barium: Potentially useful dialkyls of the heavy alkaline earth elements. *Chem. Eur. J.* **2008,** *14*, 11292-11295.

130. Nesmeyanov, A. N.; Sazonova, V. A.; Drozd, V. N., Azides of ferrocene. *Doklady Akademii Nauk Sssr* **1963,** *150* (2), 321-324.
131. Shafir, A.; Power, M. P.; Whitener, G. D.; Arnold, J.; Long, N. J., 1,1'-Diaminoferrocene. *Inorg. Synth.: Volume 36* **2014**, 65-72.
132. Shafir, A.; Power, M. P.; Whitener, G. D.; Arnold, J., Synthesis, Structure, and Properties of 1,1'-Diamino- and 1,1'-Diazidoferrocene. *Organometallics* **2000,** *19*, 3978-3982.
133. Kundig, E. P.; Monnier, F. R., Efficient Synthesis of Tris(acetonitrile)-(η^5-cyclopentadienyl)- ruthenium(II) Hexafluorophosphate via Ruthenocene. *Adv. Synth. & Catal.* **2004,** *346*, 901-904.
134. Dolomanov, O. V.; Bourhis, L. J.; Gildea, R. J.; Howard, J. A. K.; Puschmann, H., OLEX2: a complete structure solution, refinement and analysis program. *J. Appl. Cryst.* **2009**, *42*, 339-341.
135. Sheldrick, G. M., SHELXT - Integrated space-group and crystal-structure determination. *Acta Cryst. A Foundation and Advances* **2015**, *71*, 3-8.

For Table of Contents: